Available on CMS information server

CMS NOTE -2007/024

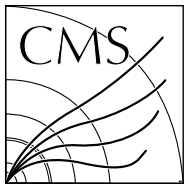

The Compact Muon Solenoid Experiment

CMS Note

Mailing address: CMS CERN, CH-1211 GENEVA 23, Switzerland

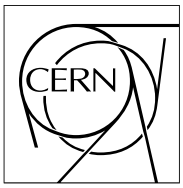

6 March 2007

Simulation of Cosmic Muons and Comparison with Data from the Cosmic Challenge using Drift Tube Chambers

P. Biallass, T. Hebbeker, K. Hoepfner

Abstract

The reconstruction of cosmic muons is important for the commissioning phase and alignment of the Compact Muon Solenoid experiment (CMS), in particular during the early phases of operation with physics collisions. In this context the Magnet Test/Cosmic Challenge (MTCC) with its comprehensive cosmic data taking periods including the presence of the magnetic field has been like a dress rehearsal of detector hardware and software for the upcoming startup of the CMS detector. In addition to data taking also the comparison with simulated events is a crucial part of physics analyses. This study introduces a new cosmic muon generator, CMSCGEN, and it presents its validation by comparing with data from MTCC. As an example results from a reconstruction study using the barrel Muon System are shown, comparing data and Monte Carlo prediction at the level of single chambers up to reconstructed tracks including momentum measurements.

1 Introduction and Motivation

During the assembly and the commissioning of different parts of the Compact Muon Solenoid (CMS) experiment, cosmic muons are the only available source of high energy particles that can be used for tests. As CMS is pre-assembled on the surface, the rate of cosmic muons traversing the detector is high enough to enable high statistics tests during a relatively short period of time. Thus cosmic muons are an ideal source for extensive checks of detector hardware, readout electronics, data acquisition and even reconstruction algorithms.

The test of the CMS magnet in summer 2006 provided an unique opportunity to test also the CMS detector since the iron return yoke, and thus the entire detector, had to be closed to allow the operation of the magnet. A dedicated cosmic data taking period – the Magnet Test and Cosmic Challenge (MTCC) – has taken place between June and November 2006 using subsets of the CMS sub-detectors. Apart from integration issues, recording of cosmic muon tracks with and without magnetic field was a goal. This test accomplished to record more than 230 million events, to run the detector in stable mode for more than 2 months and to achieve the nominal B=4T magnetic field. The Cosmic Challenge can be regarded as a very promising dress rehearsal for the upcoming start up of the Large Hadron Collider (LHC).

Another important aspect of the Cosmic Challenge is the coincidence in time with the availability of the new reconstruction software package in CMS, CMSSW. The Cosmic Challenge also offered an extensive test of this important new development. It gave the opportunity to gain experience handling real data and to investigate the performance of the reconstruction algorithms using data.

This study completes the full chain from data taking to the final data analysis by comparing cosmic data recorded with the CMS detector to predictions obtained from simulation. In order to achieve this goal a new cosmic muon generator, CMSCGEN, has been developed and included in the CMSSW-packages. Two dedicated high statistics samples, with and without magnetic field, have been produced in order to validate the Monte Carlo prediction of the generator and the subsequent detector simulation, comparing them with data recorded during the MTCC. Results of these comparisons and general reconstruction studies are presented here. We focus on the reconstruction of cosmic muons using the Drift Tube chambers of the CMS Barrel Muon System [1]. The gained experience is also of great interest for the future as cosmic muons are an important instrument of monitoring and aligning the CMS detector during LHC operation.

2 The MTCC Setup and the CMS Muon System

During the MTCC, parts of all CMS subdetectors have been operated and read out simultaneously, ranging from inner tracker modules to some crystals of the Electromagnetic Calorimeter and sectors of the Hadronic Calorimeter, up to a considerable number of muon barrel and endcap detectors.
For the Muon System, detector installation and commissioning is ongoing and a subset of these detectors sufficient to achieve the goals has been operated for the MTCC, including final cabling and final electronics. From the installed muon barrel detectors – Drift Tube chambers (DT) and Resistive Plate chambers (RPC) – three instrumented sectors were read out in the two positive barrel wheels, in wheel YB$+2$ the bottom sector 10 along with its adjacent sector 11 and in wheel YB$+1$ only sector 10 (see Fig. 1). This accounts for 14 DT chambers of type MB1/MB2/MB3/MB4 and 21 RPC chambers (note that station 4 in sector 10 is split in two chambers), corresponding to about 10000 Drift Tube channels.

The basic detection element of a Drift Tube chamber is a $42\ \mathrm{mm} \times 13\ \mathrm{mm}$ drift cell (wire-length $\approx 2.5\ \mathrm{m}$, depending on chamber type) filled with an Ar/CO_2 gas mixture. Four layers of staggered drift cells form a group, called a Superlayer (SL), with three Superlayers making up a chamber, in total 12 layers of drift cells. The bending of the muon trajectory in the r-φ plane of CMS is measured by the two ϕ-SL while the third, the θ-SL, determines the perpendicular coordinate in the r-z plane. A honeycomb pannel of $128\ \mathrm{mm}$ thickness placed between the θ-SL and one ϕ-SL gives rigidity and a bigger lever arm to the ensemble. The only exception of this scheme are the outermost MB4 chambers containing only two ϕ-Superlayers.

In the MTCC a subset of the final readout and trigger electronics [2] has been operated for triggering and data taking – that is a ReadOut Server (ROS) and a Trigger Sector Collector (TSC) per sector, three of each in total, installed on the towers near the wheels. Connected via $130\ \mathrm{m}$ long optical fibers, three Drift Tube Track Finders (DTTF) were used in the counting room, along with a Wedge Sorter (WS) and a Barrel Sorter (BS) in order to generate the Level 1 trigger information provided to the CMS trigger system. Apart from the DT system, also the Forward Muon System and the barrel RPC could provide a first level trigger, including multiple triggers for example of barrel DT and RPC detectors. The trigger input was processed and distributed to CMS by the Local

Trigger Control (LTC) which assigned a trigger bit for the sub-detector generating the trigger. This information was part of the data stream and could be used to select events triggered by, for example, Drift Tube chambers.

The muon barrel trigger electronics are designed to select high p_T muons originating at the interaction point of pp-collisions. In the MTCC, where cosmic ray muons mainly from above are traversing the detector, the trigger logic had to be modified. The angular acceptance per chamber was maximal in order to allow for muons arriving from all directions and not only from the interaction point. The on-chamber trigger electronics required either two high quality track segments (4 hits) in both ϕ-SLs or the combination of one high quality and a low quality segment (3 hits) in both ϕ-SLs (HH and HL trigger configuration). Both ϕ track segments are correlated by the TRAck COrrelator (TRACO) which is a key element of the trigger electronics mounted directly on the chamber. The DTTF, WS and BS did not select muons based on their momentum and quality, as it is designed to be at LHC operation, but simply issued a trigger when two Drift Tube chambers recorded a track segment.

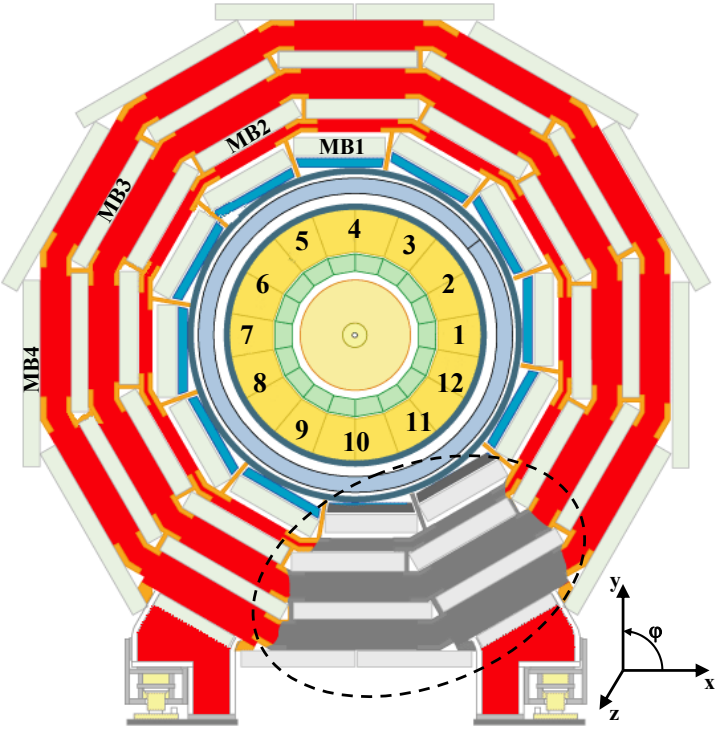

Figure 1: *The MTCC exploits in the barrel region three sectors in the wheels YB+1 (sector 10) and YB+2 (sectors 10, 11) instrumented with Drift Tube chambers and Resistive Plate chambers. Here global z is along the beam line.*

3 CMSCGEN – A New Cosmic Monte Carlo Generator for CMS

This new cosmic generator has been included in the CMSSW software package since version 0_7_0, which enables the user to simulate cosmic muons for a detector on surface as well as in the underground cavern. It has replaced a previous generator [3], re-using a large part of the infrastructure from the old generator but improving some of the extrapolation features and its performance when compared to real cosmic data. In particular the dependency on the incident angle is now more accurate and the estimate of rates more realistic. The changes made are almost transparent to the user as only the physical input of the generator has changed. A first study using the old generator can be found in [4].

As an overview, cosmic muons arrive at the surface of the earth (assumed locally flat) with an energy dependence of $\mathrm{d}N/\mathrm{d}E \propto E_\mu^{-2.7}$, their angle off the vertical axis can be described by $\mathrm{d}N/\mathrm{d}\theta_y \propto \cos(\theta_y)\sin(\theta_y)$, and their angle in the horizontal plane ϕ_{xz} is uniformly distributed (see Fig. 2 for definition of angles). In reality energy E and incident angle θ_y are correlated and the energy dependence becomes even steeper with increasing energy, see [5].

In order to model a realistic cosmic muon spectrum, dedicated parameterizations of energy dependence and incident angle have been used, also accounting for an energy dependence of the incident angle. These parameter-

izations have been adopted from L3CGEN [6], a cosmic muon generator developed for the L3+Cosmics experiment [7]. The original parameterizations have been obtained from the CORSIKA program version 5.20 [8], a program widely used for the simulation of extensive air showers, and have now been included in the CMSSW-package of CMSCGEN. For detailed information on the parameterizations see [6]. Note that the results of the L3+Cosmics experiment also represent an initial validation of the parameterizations implemented in the generator since they have been successfully used for several studies, e.g. [9] and [10]. In addition to this a quick check at the generator level can be performed, determining the spectral index of the energy distribution at $100\ \mathrm{GeV}$ for vertical cosmics: Using CMSCGEN one can obtain a dependency $\mathrm{d}N/\mathrm{d}E \propto E^{-3.09\pm0.05}$ which is compatible with the value of the exponent 3.11 ± 0.03 from [11].

Cosmic muons at sea level have a charge ratio $N_{\mu+}/N_{\mu-}$ which is bigger than one. This excess of positive muons is caused by the charge of the primary cosmic radiation arriving at the earth which are protons essentially. This surplus is reduced by interactions in the atmosphere, so that in the end a ratio not far from unity can be observed. As the correlation with energy and angle is not strong, an average of $N_{\mu+}/N_{\mu-} = 1.33$ is used in the generator.

Another property in which cosmic muons differ from muons produced during pp-collisions is the timing uncertainty. As they arrive at random times and are not bunched, the exact approach time at different sub-detectors is not known. Still the CMS detector is read out in a clock cycle of $25\ \mathrm{ns}$, so that the starting time of the cosmic muons is distributed uniformly between $-12.5\ \mathrm{ns}$ and $12.5\ \mathrm{ns}$. The generated starting time of the cosmic muons is chosen randomly in this interval in order to account for the timing jitter.
In the process of generation the cosmic muons are produced on a flat surface, assuming the properties of cosmic muons at an altidude of $470\ \mathrm{m}$ above sea level (corresponding to the surface of the L3 site, CMS surface is very similar with $510\ \mathrm{m}$). They are then extrapolated as straight lines either to the underground cavern $90\ \mathrm{m}$ below the ground (including the simulation of energy loss in rock, wall and air) or to a detector setup on surface without any energy loss during propagation. Only the cosmic muons hitting a cylinder with $R = 8\ \mathrm{m}$ and $Z = \pm 15\ \mathrm{m}$ around CMS are selected and passed on to the rest of the simulation chain, using the default detector simulation inside CMSSW. The vertex of the cosmic muon is placed on this cylinder and its momentum vector contains the generated angles and energy of the cosmic muon.

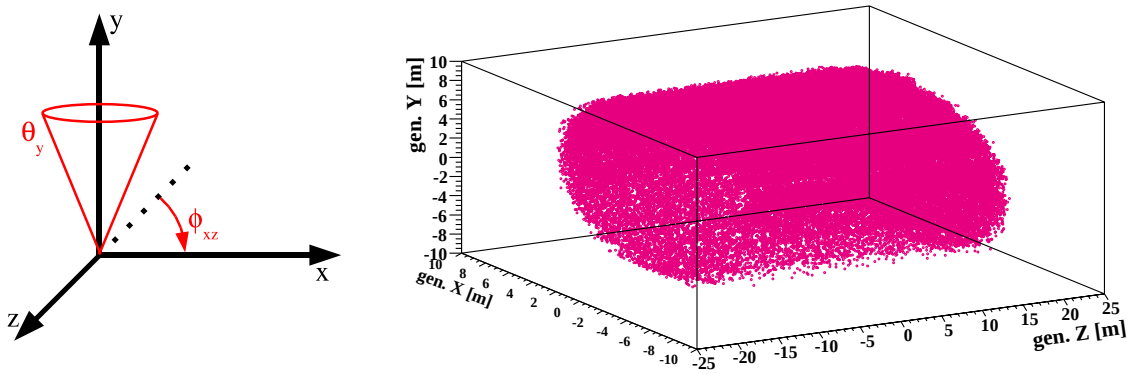

Figure 2: *Left: Definition of angles which can be specified when configuring the cosmic muon generator. The coordinate system represents the global CMS one, thus the z-axis is parallel to the beam line.*
Right: The position of the generated vertices of 1 million cosmic muons is shown. The cosmic muons are on the surface of a cylinder around CMS which is the starting point before they are traced through the material and magnetic field by the detector simulation.

3.1 Kinematical range

Using the input from L3CGEN it is now possible to simulate cosmic muons down to lower energies than before and with higher accuracy. The user can choose within the energy range of $2\ \mathrm{GeV} - 10000\ \mathrm{GeV}$ and incident angles up to $\theta_y = 88°$. Note that the angles above $75°$ represent only extrapolations of the parameterization, thus the results are expected to have slightly larger errors. In general an uncertainty of 5% between used parameterizations and original predictions from CORSIKA can be expected in the energy range between $10\ \mathrm{GeV} - 1000\ \mathrm{GeV}$. Note that below $10\ \mathrm{GeV}$ geomagnetic effects and solar influences play a significant role (see [11]) and further increase the uncertainty. Below $2\ \mathrm{GeV}$ the energy and angular dependencies of cosmic muons change dramatically and new physical interaction processes set in. Thus the simulation of even smaller energies cannot be described by

this generator and much more complicated parameterizations must be developed. Still a $2\ \mathrm{GeV}$ cut-off is highly sufficient to model the cosmic muon spectrum expected during MTCC on surface or during LHC running in the underground cavern.

Fig. 2 shows the definition of the angles which can be chosen to model a certain cosmic muon spectrum. As an example for the generated distributions, the output of 1 million cosmics generated in ROOT-interactive mode can be seen in Fig. 2 and Fig. 3, using the full kinematical range and assuming a CMS detector on the surface. The first plot shows the position of the generated cosmic vertices which reside on the cylindrical surface around CMS. The other plot depicts the kinematical properties of the cosmic muons. One can nicely see the steep energy dependence and the suppression of small incident angles due to a vanishing spatial angle at almost vertical cosmics. The modulation in ϕ_{xz} can be explained with the cylindrical surface of the CMS detector, which is the starting point for the cosmic muons. The minima at 0° and 180° correspond to the endcaps facing the cosmics while the maxima refer to the transition between endcap and barrel view. Note that for vertical cosmics no modulation is expected.

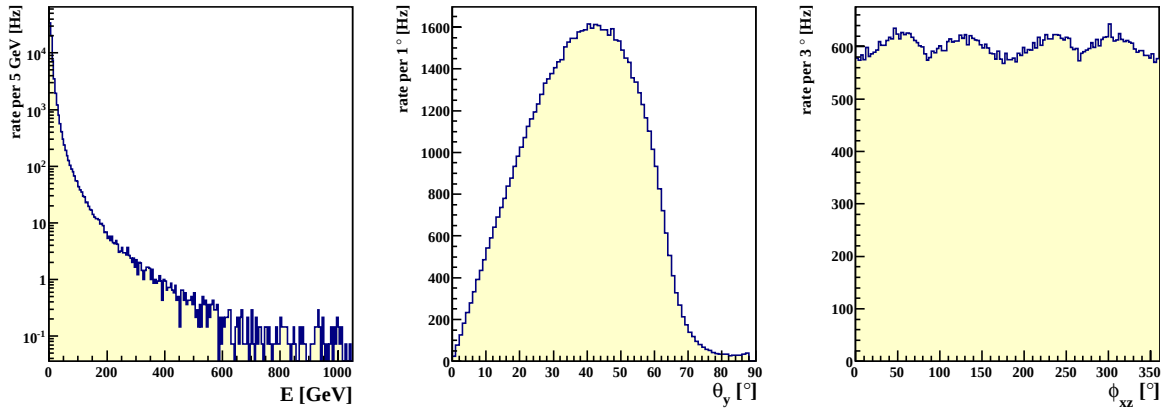

Figure 3: *The kinematical properties of* 1 *million cosmic muons generated with CMSCGEN are shown which are the output of the ROOT-interactive mode. The full kinematical range of the generator is used with an energy of* $E = 2\ \mathrm{GeV} - 10000\ \mathrm{GeV}$ *(left), an incident angle of* $\theta_y = 0^\circ - 88^\circ$ *(middle) and full* ϕ_{xz} *coverage (right).*

3.2 Generator level preselection using straight line extrapolations

As explained above the cosmic muons are generated at a plane surface and are then extrapolated as straight lines to the CMS detector. This simple extrapolation mechanism offers the opportunity to include simple preselections at the generator level. First of all it makes possible to describe energy loss in the rock above the CMS underground cavern. This can be enabled via a flag in the configuration-file called *untracked double ElossScaleFactor = 1.0*. Thus using ElossScaleFactor = 0. means simulating cosmic muons for a CMS detector on surface. In addition to this, in general two types of generator preselection can be chosen:

1. Change the dimension of the whole detector volume
2. Change the dimension of the target volume

Using option 1. means that the cylindrical surface around CMS on which the cosmic vertices are located can be shrunken. As a consequence cosmic muons which are generated on a plane are extrapolated to this newly defined cylinder. As the vertices are passed on to the detector simulation, this means that the cosmic muons may start within the CMS detector. Note that no energy loss in material of the detector and no influence of the magnetic field outside this cylinder is accounted for as the extrapolation uses simple geometrical predictions. A good example for this feature is the *untracked bool TrackerOnly = true* option which can be enabled via the configuration file. In this particular case the starting vertex of the cosmic muons within CMSSW is a cylinder around the tracker with $R = 1.1\ \mathrm{m}$ and $Z = \pm 1.1\ \mathrm{m}$. This option is very useful to create a sample dedicated for comparisons with the cosmic assembly tests of the tracker-setup before installation in the CMS detector, like the TIB/TID Slice Test.

The second option controls some target volume inside CMS which can be defined. This means that the vertices of the cosmic muons are on the default cylinder around CMS, but still the muons are extrapolated even further according to their angles and only those hitting the target volume are saved and passed on to the time consuming detector simulation and digitization. The target volume can be controlled using *untracked double RadiuOfTarget = XY [mm]* and *untracked double ZDistOfTarget = XY [mm]* in the configuration file. Again, no detector material or magnetic field effects are accounted for during extrapolation. As a consequence a target volume too small can introduce a bias, especially due to bending caused by the magnetic field in the $x-y$ plane. An additional option is to cut the default target volume (i.e. full CMS detector) in two halves in z which ensures that all simulated cosmic muons penetrate the positive wheels and end-cap. Setting *untracked bool MTCCHalf = true* in the configuration file enables this option which has been included in order to increase the statistics of the simulated sample for the MTCC. Note that still during detector simulation all material and magnetic field in the negative half of CMS are included and no bias is introduced.

3.3 Normalization of the cosmic muon flux

Another important improvement with respect to the previous generator is the absolute normalization of the cosmic muon flux which allows to predict cosmic muon rates as seen by the CMS detector. As a first step the number of cosmic muons which are originally generated at the plane surface is set in relation to a known reference flux. Using the average of various measurements, see [11], the muon flux is normalized with respect to the amount of vertical cosmics at $100\ \mathrm{GeV}$ and per sr:

$$\Phi_{norm} = \frac{\mathrm{d}N}{\mathrm{d}A\ \mathrm{d}\Omega\ \mathrm{d}E\ \mathrm{d}t} = (2.59 \pm 0.18) \cdot 10^{-3}\ \ \mathrm{m}^{-2}\,\mathrm{sr}^{-1}\,\mathrm{GeV}^{-1}\,\mathrm{s}^{-1} \qquad . \tag{1}$$

Of course this is only a suggested number to calibrate the expected rates, one can easily include different reference fluxes obtained from different measurements or simulations. The uncertainty of this flux directly translates into the systematic error of any rate estimate.
As a final step one has to correct for the selection efficiency of the generator as not all generated cosmic muons might actually hit the target cylinder around the CMS detector. As a printout of the generator the user gets the rate estimate for the full target volume as specified during generation, including statistical and systematic errors. As an example the following predicted rate correspond to the MTCC setup of the Monte Carlo sample, i.e. detector at surface and cosmics have to hit the positive z-half of CMS:

$$\text{rate}_{\text{ MTCC-setup}} = 15873 \pm 127\ (stat.) \pm 1103\ (syst.)\ \ \mathrm{Hz} \qquad . \tag{2}$$

This number refers to the complete half of the detector. For practical purposes of course only small parts of the detector are read out and only rate predictions for these sub-parts can be compared to measured rates. In order to get rate estimates for a desired subpart of the detector, one simply has to compute

$$\text{rate}_{\text{ sub-detector}} = \mathrm{N_{hit}} \cdot \frac{15873}{\mathrm{N_{events}}}\ \ \mathrm{Hz} \qquad , \tag{3}$$

where $\mathrm{N_{hit}}$ is the number of events with hits in a certain sub-detector and $\mathrm{N_{events}}$ is the number of all events in the Monte Carlo sample analysed, thus all events hitting the MTCC-half of CMS.

For additional information on the generator including technical instructions how to use the MTCC Monte Carlo samples, please take a look at the CMSCGEN TWiki Web Page.

4 Data and Monte Carlo Samples Used

For this study the data taken during run 4320 and run 4406 were used. Both runs took place at the end of MTCC phase II in October 2006 and thus are part of the very final days of the Cosmic Challenge. After a month of data taking, at this late stage many experiences and improvements in operating the magnet and the Muon System have been obtained. Thus the quality of the data can be expected to be better compared to earlier runs. Of course the results of this study represent only the final step and many runs from MTCC phase I and MTCC phase II have been looked at in order to develop the analysis and gain experiences (after phase I the tracker modules have been replaced by instruments to map the magnetic field).
In the following the characteristics of both data runs are summarized.

Run 4320:

- magnetic field $B = 0$ T
- active detectors: DT chambers and CSC chambers
- number of events: $1,844,000$
- number of DT triggers: $498,000$
- 6 DT chambers used by trigger: MB2, MB3 in sector 10 YB$+1$ / YB$+2$; MB2, MB3 in sector 11 YB$+2$

Run 4406:

- magnetic field $B = 4$ T
- active detectors: DT chambers and CSC chambers
- number of events: $1,826,000$
- number of DT triggers: $420,000$
- 6 DT chambers used by trigger: MB2, MB3 in sector 10 YB$+1$ / YB$+2$; MB2, MB3 in sector 11 YB$+2$

These two runs represent a good choice to compare real MTCC data with dedicated simulation samples as it is only possible to generate samples either with $B = 0$ T or with the nominal field of $B = 4$ T. No magnetic field map is available for other values of the magnetic field. The trigger conditions in both data runs are identical, such that the results with and without magnetic field can be compared. Only events where at least the DT trigger has fired are considered in this study, for both, data and simulated events. While for data it is inherent to the data taking, for simulated events the DT trigger conditions were modeled accordingly as described in Sect. 6. To select these events in the data the LTC (Local Trigger Control) trigger-bit was used which defines if the DT system has fired. In total for each run 4×10^5 events (triggered either by DT or CSC or by both) have been processed in this study. By requiring that at least the DT trigger has fired this total number of events is reduced to a statistics of $108,253$ inclusive DT-triggered events for the B=off run and $91,952$ inclusive DT-triggered events for the B=on run.

There are two dedicated Monte Carlo samples with large statistics available: $997,500$ events with magnetic field $B = 0$ T and $997,500$ events with $B = 4$ T.

These include generation of the cosmic muons, simulation using the GEANT [12] based detector simulation within CMSSW and finally digitization of the signal of various sub-detectors active during the Cosmic Challenge. The production was performed using CMSSW_0_9_1 and the official production tools ProdAgent, using the computing resources of the GRID Tier 2 center Aachen/DESY. The 140 GB files for each dataset have been registered in the global DBS/DLS database and are available using the GRID analysis tool CRAB.

These samples have some special features which restricts them to be used only when comparing with MTCC-data:

- In the generator the option MTCC-half is used (see Sec. 3), meaning that all cosmic muons actually hit the CMS-half with $z > 0$ m (z-axis is along the beam line). Still on their way trough the detector they may also cross parts of the other half.
- A special MTCC-like geometry is used during simulation, where the pixel detector is not present and only a fraction of the silicon strip tracker modules are included, while sub-detectors such as HCAL and muon system are complete. Since only parts of the muon system are actually read out in the MTCC, the other muon chambers have to be skipped before the reconstruction step.
- For the MTCC the detector is situated in the surface hall, and hence, energy loss in the rock above the cavern is not simulated.
- During the MTCC some sub-detectors are operated in special modes optimised for the detection of cosmics. So also in the simulation these special running-modes have to be accounted for, which leads to changes in the digitization with respect to pp-collisions (e.g. inner-tracker).

- There is a lower energy-cutoff in the Monte Carlo samples in order to increase the statistics of cosmic muons reaching the bottom part of the detector, so

$$\mathrm{E_{generated}} > 7\ \mathrm{GeV} \quad .$$

  This value has been determined optimising the amount of events likely to fire a DT trigger in the MTCC setup. Still the lower energy threshold has to be kept in mind when comparing the simulated predictions to data recorded during MTCC.

Note that only $\approx 1.5\%$ of the 1 million generated events finally satisfy the acceptance and trigger conditions of the MTCC-setup and thus can be compared to data. In order to know precisely which information can be found in the Monte Carlo samples and how it was created, the configuration files used for the production can also be found at the CMSCGEN TWiki Web Page.

5 Calibration and Synchronization

In the case of the barrel DT chambers, muon reconstruction is based on the measured electron drift-time. In that sense calibration of the chambers aims at synchronizing them such that the muon's arrival time at the certain detector is common for all stations. This calibration of drift-times has to be performed in the case of pp collisions as well, so the developed schemes can be tested using cosmic muons. In the case of cosmics, there are some additional complications: Cosmic muons arrive at random times at the detector and their kinematic properties are less constrained than muons coming from a nominal interaction point. The necessary steps of synchronization for data and generated events will be discussed in the following. All of them are carried out using the official calibration tools [13] within the DTCalibration package of CMSSW.

5.1 Calibration of the data

Timing differences in the arrival time of DT signals appear at different levels with varying granularities. Firstly, signals from the individual wires arrive with a slight variation of $\pm 5\ \mathrm{ns}$ at the TDC, caused by small differences in the chamber electronics and the different cable lengths. Using test pulses a so-called "T0"-offset for each cell can be determined such that only the real drift-times and the signal propagation along the wire can cause timing differences. For the reconstruction, these corrections are read from a SQLite [14] database and the digitized drift-times are shifted accordingly.

While the first correction is intrinsic to the chamber itself and does not change after chamber installation, the next one is a mixture of different constributions. First this offset largely depends on the cable length and latencies between the chamber and the off-detector electronics. The latencies have been modified during the MTCC data-taking in order to synchronize the subsystems with respect to each other. Then the offset depends on the time when the trigger is fired and which bunch crossing is assigned to the event. In addition to this the cosmic muon has a time-of-flight from one chamber to another, depending on the place and angle where it crosses the MTCC setup. These effects are reflected in a constant offset called "tTrig" which is determined for each Superlayer. This is done using a fit routine which identifies the starting point of the drift-time spectrum when all cells of a Superlayer are added up. The derivation of a Gaussian is matched to the rising edge of the spectrum. Using mean and σ of the Gaussian the starting point of the drift-time spectrum is determined. Details of the calibration routines can be found in [13]. Again, a SQLite database is used to save these offsets and shift all timeboxes to zero.

To summarize, the applied calibrations to ensure a common starting point for the drift-time determination are:

$$t_{\mathrm{drift}} = t_{\mathrm{measured}} - T_0\ (\text{per cell}) - t_{\mathrm{tTrig}}\ (\text{per SL}) \quad . \tag{4}$$

Noisy cells are selected and discarded prior to the tTrig-fit since they interfere with the calibration routine. In the reconstruction noisy cells are included in order to avoid any bias.

5.2 Calibration of Monte Carlo events

As described in Sect. 3, the timing uncertainty of $25\ \mathrm{ns}$ in the cosmic muon arrival is introduced during the generation of the Monte Carlo samples. In addition to this intrinsic uncertainty, also simulated cosmic muons have different timing offsets in each DT chamber. While real cosmic muons suffer from time-of-flight differences with

respect to the moment the trigger fired and from hardware latencies, simulated cosmics obtain a certain time-of-flight caused by the distance between generated vertex and each traversed chamber. In addition to this, certain offsets per chamber are subtracted during default digitization, assuming the muon to originate from the nominal interaction point. This yields a situation comparable to the real data and the same calibration tool can be used in order to determine the "tTrig" from each Superlayer. Since data and Monte Carlo events are calibrated in the same way, effects caused by the used routines should be observable in data as well as Monte Carlo prediction. No "T0"-correction per cell is needed here since no electronic latencies between different wires are included in the simulation.

Figure 4 shows the comparison of the drift-time spectrum for simulated cosmic muons and data with magnetic field, after the calibration has been performed. Here all drift cells within Superlayer $\phi 1$ of MB1 in sector 10, YB$+2$, are summed up, corresponding to the granularity of the applied calibration routine. Data are normalized to the simulated events in order to reflect the smaller statistics of the Monte Carlo sample. After proper synchronization the observed spectrum of drift-times ranges from almost 0 ns (for muons passing close to the wire) to 380 ns (or 486 Time to Digital Converter counts, one TDC count being the "hardware unit"). In order to suppress effects of noise and after-pulses, only cell hits contributing to reconstructed objects, in this case a 2D-segment built from hits of either ϕ- or θ-Superlayer (see Sect. 6), are used.
Measured data and simulation agree well and the general shape of the timebox is as expected. This fact is also important since at the location of this specific chamber a relatively large magnetic fringe field of up to ≈ 0.8 T is present. In certain areas of the chamber with such a magnetic field the drift times are increased in the order of 10 ns. Still at the level of drift-time spectra for a complete Superlayer such an effect is not visible and the detector simulation seems to describe the conditions within the chamber well.

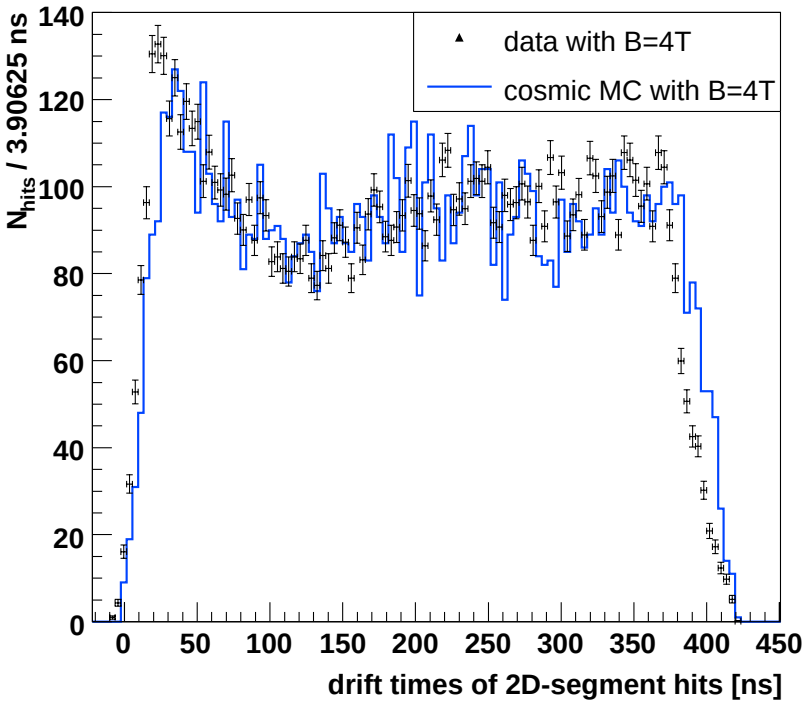

Figure 4: *In order to verify the signal creation and the signal calibration in the cosmic muon simulation, a drift-time spectrum from simulation (continuous line) is compared to drift-times as measured with real cosmic ray muons from MTCC (triangles) for hits contributing to a $2D$-segment. For this study data and simulated events with magnetic field are regarded after calibration has been performed, here for Superlayer $\phi 1$ of the horizontal MB1 of sector 10 in YB$+2$, corresponding to the granularity of the calibration routine (data normalized to MC).*

Note that the calibration routines described above still cause some remaining timing uncertainties. It is clear that the inherent cosmic jitter of 25 ns and the propagation time of the signal along the wire remain. In addition to this the constant tTrig-offset for each Superlayer is only the result of an average of many cells and many events. The obtained time-of-flight corrections are correlated with the angular distribution of the incoming cosmics and with

the geometrical acceptance of the MTCC setup. The exact sum of all offsets is specific for each event and thus can only be extracted using further information obtained during reconstruction. Such an event based correction will be introduced in Sect. 6. In this way almost the optimal resolution of the drift cells can be obtained, also when using non-bunched cosmic data.

6 Reconstruction of Cosmic Ray Muons

As in the case of calibration, also during reconstruction of cosmic muons some changes and optimizations have to be performed with respect to the default code designed to measure muons coming from a central vertex during bunched pp-collisions. While the timing uncertainty of the cosmic muons only worsens the resolution of the Drift Tube chambers, the large incident angles of the cosmic muons and the fact that they penetrate the detector from all directions causes event topologies which the default reconstruction code is not designed to handle. Therefore all vertex constraints normally used to enhance the measurement have been disabled and a dedicated cosmic track-reconstruction algorithm has been used. Also the trigger-setting has been arranged such that events with larger angles can be recorded and the acceptance is only limited by the angular reach of the trigger-electronics. Of course one cannot expect the efficiency of the trigger and the reconstruction to be equal for all event topologies. But still these modifications enable to measure almost the natural properties of the incoming cosmic ray muons, with only little bias and geometrical constraints.
In the case of data from the Cosmic Challenge, CMSSW_1_1_0 has been used to process the recorded events, while for the simulated events a previous version, 1_0_6, has been chosen. The reason for this difference is that a change in geometry has been performed between both versions. So for real data the corrected geometry is used while for simulation the one compatible with the version the sample has been created with has to be applied. Despite the differences in geometry which do not affect the physical output of this study the rest of the reconstruction chain is identical so that data and Monte Carlo prediction can be compared.
In the following the different reconstruction steps including the modifications used with respect to muons from LHC running are discussed, ranging from single cell hit reconstruction to complex track-fits. In general all 14 DT chambers active during MTCC have been used for local reconstruction as well as track reconstruction.

6.1 Local reconstruction at chamber level

Drift-times are the measured magnitudes used in the Barrel Muon System. Given the inherent imprecision of cosmic muons a linear time-to-drift relation is used in this study. This simplification assumes a perfectly homogeneous electrical field inside the cell volume which is an approximation. Influences of the magnetic field inside the muon chambers and non-perpendicular angles of the muons are neglected in this approach. Still these effects are of second order and especially for perpendicular incidence the differences between linear time-to-drift and a more detailed parametrization of the cell behaviour are small [15]. Using the linear approximation it is possible to reconstruct the one-dimensional position of the traversing muon:

$$x_{\text{hit}} = v_{\text{drift}} \cdot t_{\text{drift}} \qquad , \tag{5}$$

where a drift velocity of $v_{\text{drift}} = 54.3\ \mu\text{m/ns}$ is applied.

In the case of the simulated events, an additional step is performed during cell hit reconstruction. Since the MTCC-geometry used contains more Muon Chambers than were actually read-out with the real setup, only cell hits belonging to the actual MTCC-setup are selected and passed on to the rest of the reconstruction chain.

Still the left-right ambiguity with respect to the wire cannot be solved at the stage of single hit reconstruction. Different cells in different layers have to be combined to form 2D-segments within one Superlayer. The name implies that these segments contain a two-dimensional information, bearing in mind that the wires of a ϕ-Superlayer run perpendicular with respect to a θ-Superlayer. The segment reconstruction performs a linear fit combining the cell hits of the 4 contributing layers. Using pattern recognition and χ^2-minimization the best possible combination of cells can be determined and this angular information solves the left-right ambiguity.
The default CMSSW segment reconstruction includes vertex constraints for ϕ- as well as θ-Superlayers. These have been disabled so that all possible angles of the segments can be measured, given that the trigger has accepted the event. As a consequence in some topologies the left-right ambiguity can no longer be solved uniquely simply by choosing the segment candidate with the smallest χ^2. This can lead to segments with unphysical angles even larger than the acceptance of the trigger. In addition to these misreconstructed segments there is also a candidate which corresponds to the true path of the cosmic muon. In this case both candidates are kept and the decision

which one is correct is passed over to the following track-reconstruction step. Using the information of several DT chambers, wrongly measured segments can easily be discarded.

As introduced in Sect. 2 a Drift Tube chamber consists of 2 ϕ-Superlayers which are staggered around a single θ-Superlayer. Since the orientation of the wires in each Superlayer type is perpendicular to each other the local x-z coordinates can be measured in the ϕ-SL (φ-plane) while the local x-z coordinates are provided by the θ-SL (ϑ-plane), see Fig. 5. The angles φ and ϑ are in this case the normal spherical coordinates of the global CMS coordinate system (z along the beam line). The sectors of the Muon System are orientated cylindrically around the global z-axis. Thus for muons coming from the nominal interaction point the angles measured by an individual Superlayer, which are projections in the local reference frame only, almost correspond to the global φ- and ϑ-angles.

The final step in local chamber reconstruction is the combination of the 2-dimensional information of each Superlayer type in order to obtain 3-dimensional chamber segments. For the θ-Superlayer one can simply copy the segment information obtained before. Any further updates of the contributing hits will be discussed below in the event based correction. For the ϕ-view the 2 Superlayers are combined to form a "Superphi-segment", using all 8 contributing layers. Here the segment is refitted using the original hits of both 2-dimensional segments, thus avoiding any bias from the previous reconstruction steps. Finally θ- and ϕ-views can be combined to form a 3-dimensional chamber segment. Of course different segment candidates can be present and different combinations of them are possible. In order to limit the combinatorics and the amount of chamber segments per event, a cleaning algorithm based on the number of hits and the χ^2 of the fit is applied in order to reject poor segments. Further details on segment reconstruction within CMSSW can be found in [13].

Figure 5 shows an example of chamber reconstruction in a data event where the nominal magnetic field of 4 T is present. One can see the r-φ view of the CMS-detector. The red lines correspond to the Superphi-segments of the DT chambers. Even without proper track-reconstruction the combination of the 4 chamber segments shows a cosmic muon going through the bottom sector 10 of the detector, being bent by the magnetic field according to its momentum adn charge. The green horizontal bars correspond to segments found in the orthogonal r-z view.

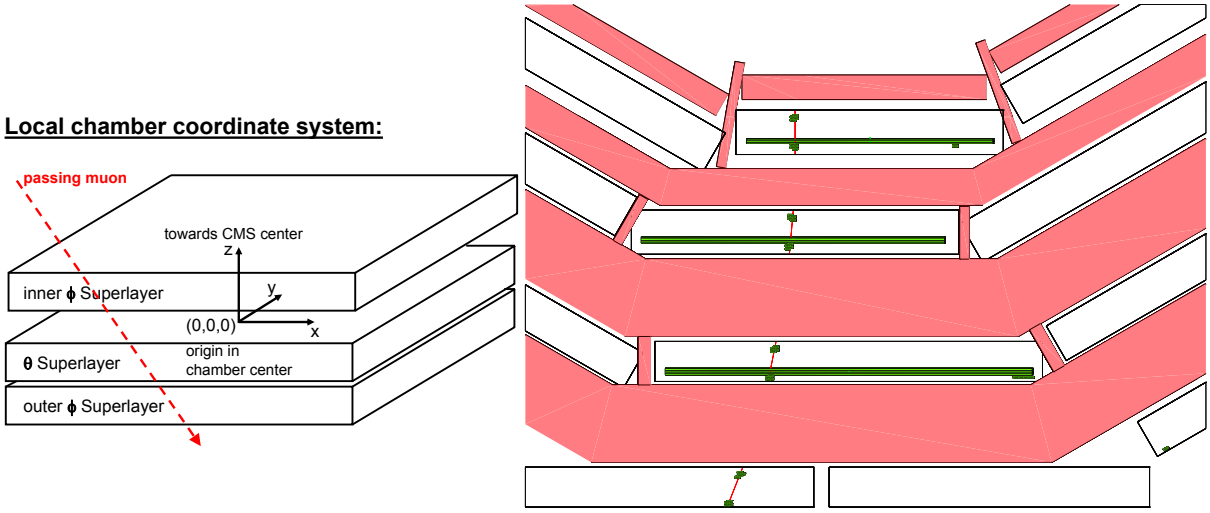

Figure 5: *Left: Definition of the local DT chamber reference frame with its origin in the center of the chamber (local y is along global z).*
Right: Iguana [16] event display from MTCC data with magnetic field of $B = 4$ T , here the r-φ view of the CMS detector is shown. The red lines indicate reconstructed chamber segments, the greenish lighted rectangles correspond to individual cells with a hit. The θ-Superlayers do not provide information for this projection, thus their measurements are displayed as green bars only (corresponding to the θ-wires). The bending due to the magnetic field can easily be seen.

6.2 Event based correction

As discussed in Sect. 5 the Drift Tube chambers have been synchronized so far assuming a constant offset. This "tTrig" accounts only for an average latency which can be subtracted from all measured drift-times. Still the uncertainty caused by the random arrival time of the cosmics can only be corrected if the additional information of reconstructed segments is available. The default segment reconstruction performs a simple linear fit, thus determining a space point and the 2-dimensional direction of the cosmic muon track for each Superlayer. In order to increase the precision of the measurement for cosmic muons a dedicated refitting-algorithm has been developed within CMSSW, for detailed information see [17].

The basic idea is to modify the linear time-to-drift relation, assuming that for each single event all hits contributing to the segment have the same latency-offset and see the same drift-velocity:

$$x_{\text{hit}} = v_{\text{drift}} \cdot t_{\text{drift}} \quad (6)$$

$$= (v_{0\ \text{drift}} + \delta v_{\text{drift}}) \cdot (t_{0\ \text{drift}} + \delta t_{\text{drift}}) \quad . \quad (7)$$

Here $t_{0\ \text{drift}}$, corresponding to Equation 4, is already corrected for the constant tTrig-offset. The value $\delta t_{\ \text{drift}}$ is different for each event (or segment if more than one are present), depending on the distance of the track from the readout electronics since the signals propagation along the wire can take up to 7 ns. More important, the arrival time of the cosmic muon with respect to the 40 MHz clock adds to this correction. On the other hand $\delta v_{\ \text{drift}}$ fine-tunes the used drift-velocity for each segment since this can be affected by the quality of the gas inside each chamber and by the intrinsic influence of the magnetic fringe-field inside the chambers, see [18]. If the angles of the incoming cosmic muons are not too large the assumption that the correction in drift-times and drift-velocity are the same for all hits contributing to one segment is well satisfied.
Using the event based correction a 4 parameter fit is performed if at least 5 hits are available (in the case of combination of the two ϕ-Superlayers). By trying to minimize the residuals, i.e. distance between measured hit-position and hit-position predicted by the segment-algorithm, a system of 4 linear equations is solved. This determines the optimal choice of the 2-dimensional position and angle of the segment, of $\delta v_{\ \text{drift}}$ and of δt_{drift}. If there are less than 5 hits, e.g. for a θ-Superlayer, only a 3 parameter fit is applied, using an unchanged $v_{\ 0\ \text{drift}}$. In both cases the individual cell hits are updated according the changes in drift-time and drift-velocity and the segment is refitted again, resulting in the optimal measurement of segment-direction and -position.

6.3 Modelling the DT-trigger setup for the Monte Carlo events

The Monte Carlo sample generated to be compared to data from the Cosmic Challenge includes the full detector simulation, so the reconstruction should perform similar in data and in Monte Carlo events. However, a trigger simulation corresponding to the special MTCC trigger setup could not be included, since it was not available at the time. Efforts have been made to manually account for the trigger efficiency.
First the geometrical acceptance of the Drift Tube chamber is accounted for. As mentioned in Sect. 4 the two chambers MB2 and MB3 of all three active sectors were included in the trigger conditions of both runs. The Drift Tube trigger during MTCC requires a coincidence of two chambers, while each chamber has to detect a correlated signal of both ϕ-Superlayers. This yields the following "pseudo-trigger" condition which have been applied both in the data and in the Monte Carlo events (to get comparable samples):

pseudo-trigger: events with ≥ 7 hits combining both ϕ-Superlayers in at least 2 chambers from all MB2/MB3 of sector 10 YB$+1$/YB$+2$, sector 11 YB$+2$

It is clear that an event passing this criterion is within the geometrical acceptance of the chamber since it left behind multiple cell hits. Still, this does not mean that the event was indeed triggered by the real MTCC setup since the on-chamber trigger electronics has a certain angular acceptance and trigger efficiency which depends on the projection of the global φ-angle in the local y-z plane, called φ_{SL}. For large angles one expects the trigger-efficiency to drop since the hardware is designed to record muons originating from the nominal vertex (which have small angles). By computing the ratio of $N_{\text{data}}/N_{\text{MC}}$ as a function of φ_{SL} one can use the simulated events to extract the shape of the trigger-curve from the MTCC data (at this stage only shape, not an absolute scale). Here data and Monte Carlo prediction are scaled to each other only in the central region at small angles ($|\varphi_{\text{SL}}| < 10°$) since efficiency close to 100% is expected here. Afterwards the obtained shape can be used to discard the generated events according to this trigger-efficiency.

The result of this trigger study can be seen in the left plot of Fig. 6, here for φ_{SL} of MB3 in sector 10 YB+1. In order to avoid the effect of bending the samples without magnetic field are used. For this horizontal chamber a vanishing angle corresponds to a vertically incoming cosmic muon. One can nicely see a plateau and then a rapid drop in efficiency at larger angles. Efficiencies larger than 100% may appear if a bin contains more data than simulated events since both are normalized with respect to each other. Also compare this to the expected trigger-efficiency obtained from trigger emulation studies, see dotted line "correlated" at the right plot in Fig. 6.

For the simulated cosmic events the shape is approximated by straight lines, with the minima at $\pm 50\,^\circ$ and the plateau between $\pm 30^\circ$. The simulated events are corrected for this efficiency shape, discarding events accordingly. Without accounting for the trigger-efficiency the tails at large φ-angles would be more prominent in the Monte Carlo prediction than in the data, also when looking at track-reconstruction.

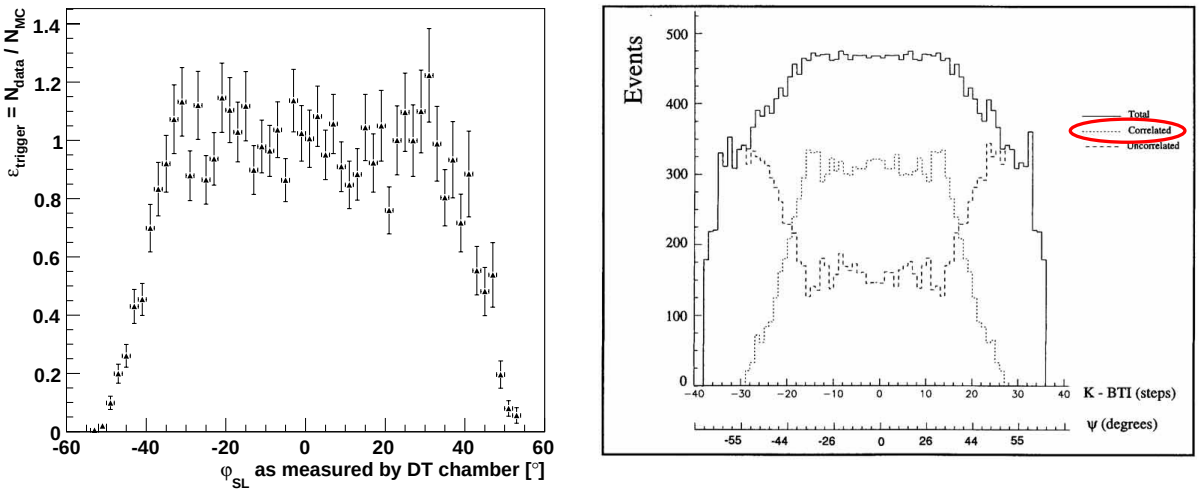

Figure 6: *Left: Trigger-efficiency-shape from MTCC data and MC in comparison, here for φ_{SL} of MB3 in sector 10 YB+1 using data and Monte Carlo samples without magnetic field.*
Right: Simulated response of the track correlation algorithm (TRACO) as a function of φ_{SL} angle, muons were generated flat in angle (from Muon TDR [1]). Correlated means that the segments of both ϕ-Superlayers match.

6.4 Cosmic track-reconstruction combining chambers

A dedicated cosmic track-reconstruction algorithm has been developed within CMSSW, a package called CosmicMuonSeed and CosmicMuonProducer (see [19] for detailed information). The motivation has been to provide a tool optimized for the cosmic data taking periods during Cosmic Challenge and during detector alignment in the early runs of LHC pp-collisions. In both cases cosmic muons are an important particle source to commission the detector and use tracks to align its components. Again, we focus on the track-reconstruction using DT chambers as an example. Reconstructing "global" muon tracks is beyond the scope of this study, even though incorporating information from tracker or end-cap muon chambers is also possible.
This new algorithm assumes muons to come from "outside" the detector and it excludes the implicit vertex constraints which are used in many steps of the standard tracking software. As a starting point the 3-dimensional chamber segments of the local reconstruction are used for seed-finding. Since all vertex constraints have been already disabled there and since the actual direction of the segment is used, it is possible to efficiently find muon tracks passing the MTCC setup from various directions.
The next step consists of the actual track-fit. Starting from the seed and using a Kalman-filter technique [20] the segments of the different Drift Tube chambers are combined. The general procedure is to use the measured segment-position and -direction and extrapolate to the next muon station, assuming a certain momentum estimate. This results in a predicted state in which the influences of energy loss in material, magnetic field and multiple scattering are included. This predicted state can then be combined with the measured values, forming a weighted average of both measurement and prediction.

In this study a forward-fitter is used combining the 3-dimensional chambers segments, starting from inside-out (MB1 to MB4). Afterwards a backward-fitter is applied with a finer granularity, this time using the measurements of individual cell hits. The propagator used so far in the algorithm is the Stepping-Helix-Propagator which is tuned based on information from simulation (Geant4E) as well as from the first principles of the passage of particles

through matter. In the end it is possible to access the track parameters, i.e. position/direction/energy, at the innermost and outermost measurement, e.g. MB1 and MB3. The common tracking angles used are defined in Fig. 7. A schematic drawing of the track-fitting procedure without the presence of a magnetic field is also shown.

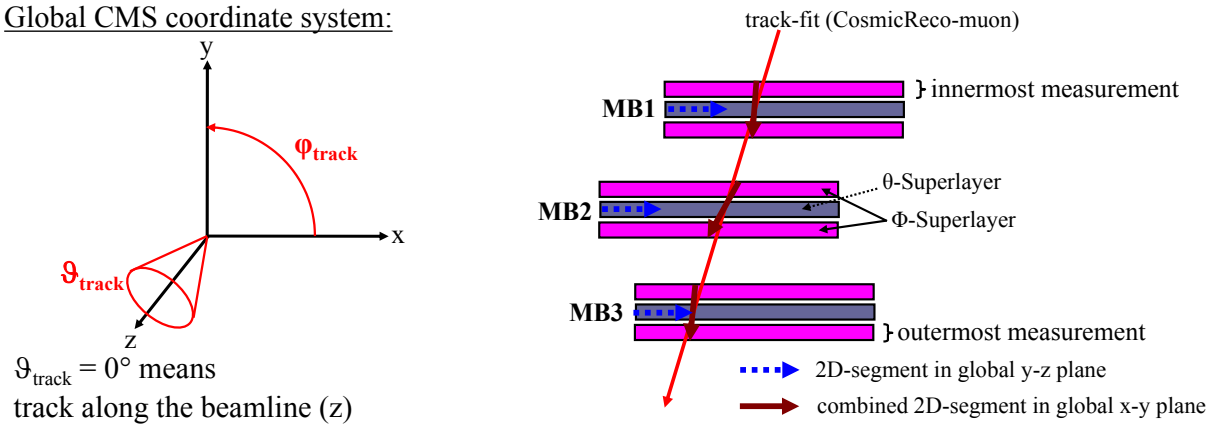

Figure 7: *Left: Definition of the angles used during track-reconstruction within the global CMS coordinate system.*
Right: Illustration of the combination of several DT chamber measurements resulting in a track-fit. In this projection only the ϕ-Superlayers contribute to the measurement. Since no magnetic field is present the final track is a straight line and the track-parameters can be accessed at the innermost and outermost point.

7 Results

In this section several plots will be presented which illustrate this first data-Monte Carlo comparison using the barrel Muon System of CMS. The output of this study aims at different aspects.
First of all the comparison with the real world, i.e. data coming from the detector, serves as an important validation of the cosmic muon generator. If general properties such as angular distributions or energy of the cosmic muons measured by the detector match in data and in simulation, then this means that the assumed parameterizations which are the input to CMSCGEN can describe nature to a satisfying degree. Even though for many results of the L3+Cosmics experiment these parameterizations have already been used (e.g. [9], [10]), it is important to study their correctness also with the final code used in CMSSW.
Then of course the intrinsic cosmic distributions are not directly measured by the detector. The observed distributions are strongly influenced by the geometrical acceptance of the MTCC setup, the efficiency of the hardware and by the physical processes which take place inside the muon chambers. Thus the next important check when comparing to measured data is the correctness of the detector simulation and the modelling of the different subdetector parts. One has to bear in mind that in the beginning of LHC-running CMS will undergo an extensive period of detector calibration and understanding its performance, which will result in a more realistic tuning of the simulation. Even though the results presented here use cosmic muons only, still they give first hints of how well the data can be described by the simulation and they give cross-checks to spot bugs in the software from early on. Another advantage of using simulated events is that one can access the generated properties of the particle and thus can compare in detail the differences between reconstructed and expected values. So to compare distributions in data and Monte Carlo is one thing, but in order to conclude that the reconstruction software is working properly and to judge its performance, accessing the generated information of particles is essential.
Finally simply the fact that a complete analysis chain has been performed is a very important achievement. Numerous steps have to be done, starting from the operation of the detector and the data-taking, transferring them to the computing sites, producing a Monte Carlo sample with comparable conditions and analysing both data and Monte Carlo events with the official reconstruction software. Many problems have to be solved along the way and many lessons can be learned. Of course the plots which will be shown do not reflect the full picture, they are the result of the work of countless people at different levels of the experiment and they give proof of the fact that CMS is ready for physics analyses with LHC-data.

7.1 Results from local reconstruction

As introduced in Sect. 6 local chamber reconstruction combines the different cell measurements of all layers of a single Drift Tube chamber. Since the θ-Superlayer and the two ϕ-Superlayers can be combined to provide a 3-dimensional chamber segment, even at this level the angular properties of data and simulated events can be tested. For all the following results events have been selected where only a single chamber segment has been found per chamber. This reduces the effect of multiple segment candidates due to noise hits and to different combinatorial possibilities given the lack of a vertex constraint. In addition to this the segment is required to contain ϕ- as well as θ-information.

A very characteristic quantity is the incident angle θ_y of the cosmic muons. The definition of the angle has been presented in Fig. 2 and the generated angle has been already shown in Fig. 3. This now can be compared to the reconstructed incident angle as measured by the horizontal MB3 in sector 10 of wheel YB+2, see Fig. 8. The plot shows the data with triangles in comparison with the prediction of the simulated sample as the solid line. The distribution of the incident angle of the cosmic muons with and without magnetic field can be seen in the right/left plot respectively. The data are normalized to the simulated events in order to reflect the smaller statistics available.

First of all these two plots illustrate that it is possible to reconstruct the direction of cosmic muons correctly with and without magnetic field. Secondly the agreement between data and MC prediction is very good, the general shape of the distribution is reproduced nicely and looks very similar to the generator output, see Fig. 3. This means the assumed parameterizations of the generator CMSCGEN are correct and that the detector simulation works well. Compared to the generator information the reconstructed angle in data as well as Monte Carlo drops much sharper after $\approx 30°$. This reflects the limited acceptance of the chamber geometry and the trigger-setup. Since DT chambers are designed to measure muons coming from the nominal interaction point they are not optimised for large angles. Without modelling of the trigger as described in Sect. 6 the agreement between data and Monte Carlo prediction at large angles would be much worse. Still the slight excess of simulated events around $50\,°$ could be due to the imperfect description of the actual trigger. Another important aspect is the comparison with and without magnetic field. One can see that the general shape of the distribution is only slightly affected by the presence of the $4\,\mathrm{T}$ magnetic field, the right plot appears only a bit sharper. More important is the reduction (80%) of reconstructed muons in the presence of the magnetic field, the reason being that cosmic muons are deflected on their way through the detector so that they no longer reach the MB3 of the bottom sector.

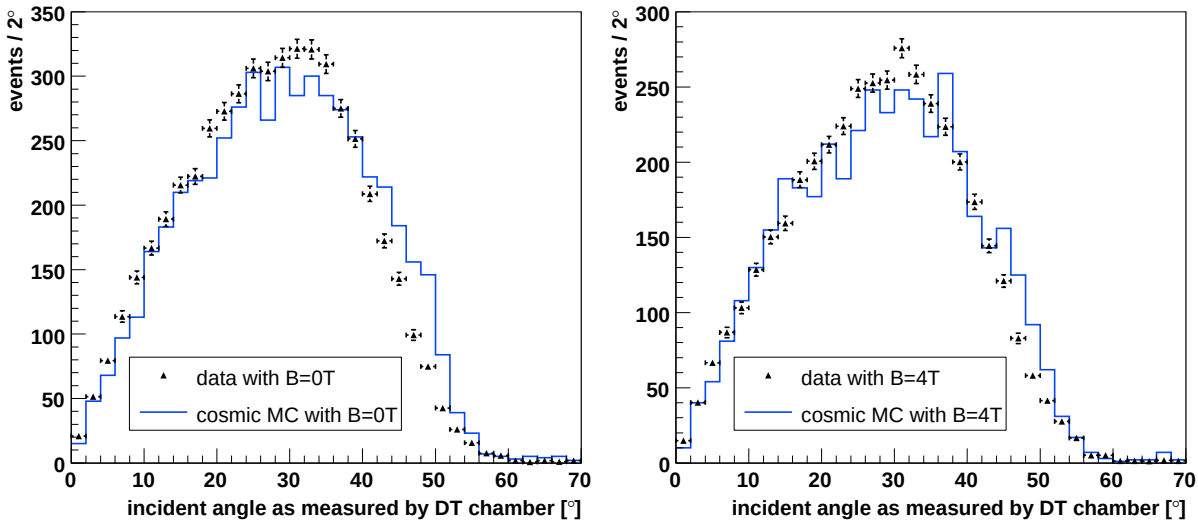

Figure 8: *Incident angle of the cosmic muons as measured by local chamber reconstruction, here for horizontal MB3 in sector 10, YB+2. Data and MC prediction can be compared, without magnetic field (left) and with magnetic field (right). In both cases the data are normalized to the simulated events (continuous line).*

Correlated with the angular dependencies of the incoming cosmic muons is also the number of muons crossing two wheels or crossing two sectors. These specific events are important for alignment studies since they contain important information to determine the relative position of sectors and wheels with respect to each other. In general

each of the 3 sectors read-out during the Cosmic Challenge sees $\approx 1/3$ of the triggered events, in the data as well as in the Monte Carlo sample. So the sectors are almost equally illuminated. From all events with magnetic field fulfilling the trigger conditions only 7% in the data and 11% in the Monte Carlo prediction have 2-dimensional segments in both wheels. Only 8% of the data and 9% of the Monte Carlo events have both segments in sector 11 and in one of the sectors 10. Only this fraction of the data can be used to contribute to the global alignment of wheels and sectors.

In order to judge the correctness of the measurement and the performance of the segment-reconstruction, residuals can be studied. A residual is defined as the distance between the predicted hit position when extrapolating the segment direction into a cell and the original hit position. This quantity is very sensitive to the intrinsic cell resolution and strongly depends on the correctness of the calibration of data and Monte Carlo events, see Sect. 5. Figure 9 shows the residuals of a specific layer for a single chamber, layer 2 of Superlayer $\phi 1$ in chamber MB2 Sector 10 YB+1. Data and simulated events with and without magnetic field are shown after the following selection cuts for a segment have been applied: The directional information is taken from a "Superphi-segment" which is built using 8 hits. In addition to this an angular cut of $|\varphi_{\mathrm{SL}}| < 10^{\circ}$ is applied. This ensures that the incoming cosmic muons have small angles since it is known that the linear time-to-drift relation is comparable to the more sophisticated parameterisation only in this regime [15].

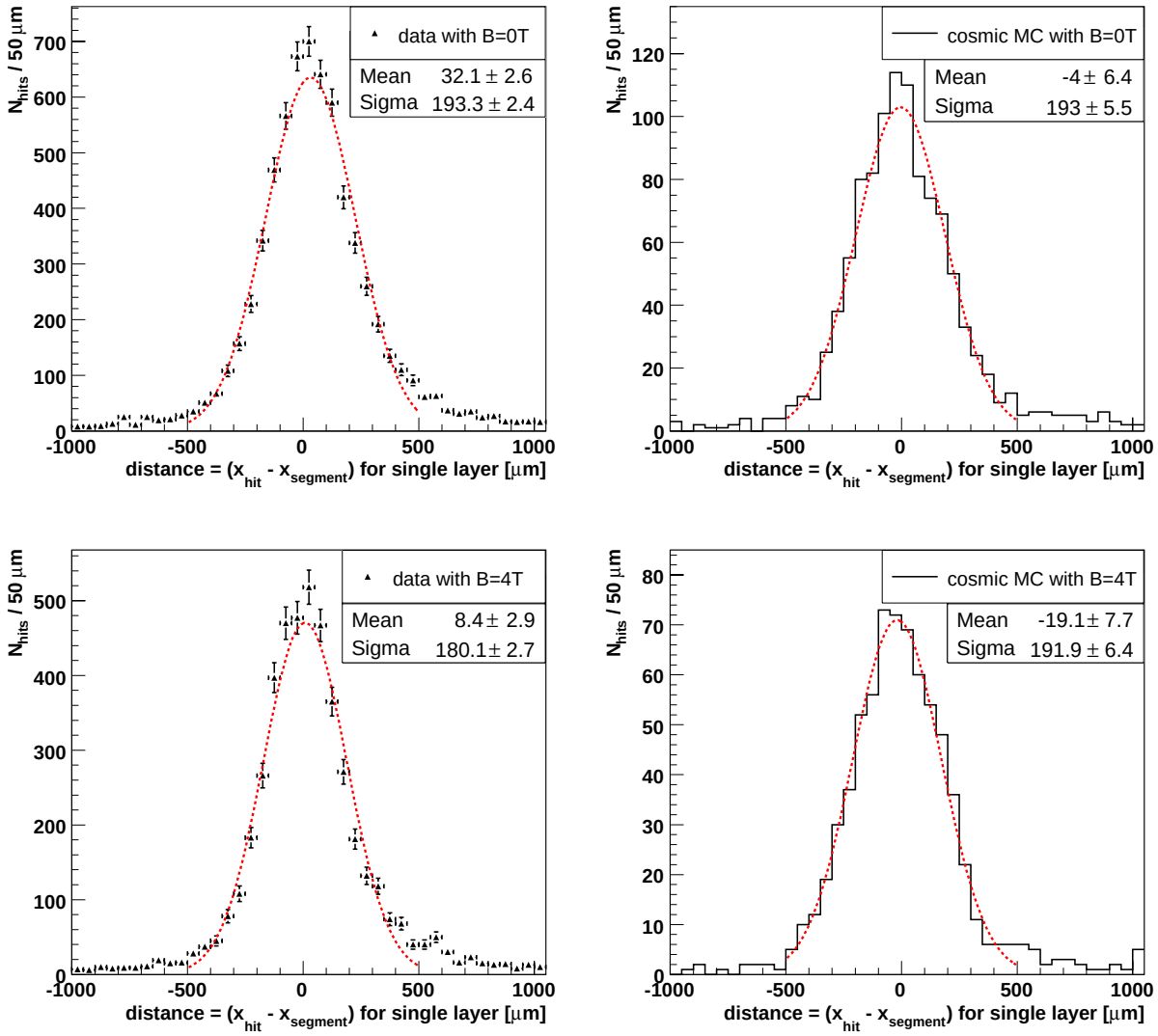

Figure 9: *The residuals for a single layer (layer 2, SL $\phi 1$, MB2, Sec 10, YB+1) are shown including a Gaussian fit. The left plot corresponds to cosmic data (triangles) and the right plots to the simulated sample (continuous line); the top row displays data and MC without magnetic field and the bottom row the case with magnetic field. Note that the used segments origin from the combination of the two ϕ-SLs with 8 hits and $|\varphi_{SL}| < 10^{\circ}$.*

All four plots are compatible with a Gaussian distribution which is centered around zero and has a sigma around $190\ \mu\mathrm{m}$. This shows that the calibration of both data and Monte Carlo samples is correct and that the reconstruction algorithm works well in all cases. Since the sigma of data and Monte Carlo distributions are comparable the detector simulation seems to model well the uncertainties of the real measurement. Note that the small sigma also underlines the importance of the event based calibration correction as introduced in Sect. 6. Without this optimization the $25\ \mathrm{ns}$ jitter of the cosmics results in widths of the residuals of $\approx 500\ \mu\mathrm{m} = \sqrt{(54\ \mu\mathrm{m/ns} \cdot \frac{25\ \mathrm{ns}}{\sqrt{12}})^2 + (250\ \mu\mathrm{m})^2}$, where $250\ \mu\mathrm{m}$ is the intrinsic design cell resolution [1] and $\sqrt{12}$ accounts for the uniform distribution of the arrival times.

Note that the observed sigma of $180\ \mu\mathrm{m}$ in the data with magnetic field does not directly correspond to the single cell hit resolution. Even though the residuals are shown only for a single layer the probed cell is still included into the segment fit and into the event based correction fit. In order to really compare the actual measurement with the predicted hit position, layer 2 can also be excluded from both fits. Thus segment direction and timing correction are determined by using only the remaining 7 hits. Still all hits are finally updated using the tTrig and $v_{\text{ drift}}$ output of the fit. Table 1 summarizes the sigmas of the residuals under different conditions in data and in simulated events with magnetic field. Using the observed values with and without the probed cell included in the fits one can estimate the true cell hit resolution of the Drift Tube chamber. Correction factors have been derived from a toy Monte Carlo performing a linear fit through 7/8 hits with their positions smeared by the design resolution of $250\ \mu\mathrm{m}$: 0.87 for the residual with the hit not in the fit and 1.17 for the residual with all 8 hits used for the fits. For the data this results in $\sigma_{\text{cell}} = 238 \pm 5\ \mu\mathrm{m}$ and $\sigma_{\text{cell}} = 211 \pm 4\ \mu\mathrm{m}$, which leads to the weighted average of $\overline{\sigma}_{\text{cell}} \approx 219\ \mu\mathrm{m}$. In the Monte Carlo prediction one obtains a very similar value, $\overline{\sigma}_{\text{cell}}(\mathrm{MC}) \approx 231\ \mu\mathrm{m}$. To summarize, all this means that using the event based correction also with cosmics one can reach the design cell hit resolution.

	hit not included in calibration- and segment-fit	hit included in both fits	extracted cell hit resolution
data with $\lvert\varphi_{\text{SL}}\rvert < 10^\circ$ and $N_{\text{hits}} = 8$	$\sigma = 274 \pm 6\ \mu\mathrm{m}$	$\sigma = 180 \pm 3\ \mu\mathrm{m}$	$\sigma_{\text{cell}} \approx 219\ \mu\mathrm{m}$
MC with $\lvert\varphi_{\text{SL}}\rvert < 10^\circ$ and $N_{\text{hits}} = 8$	$\sigma = 337 \pm 25\ \mu\mathrm{m}$	$\sigma = 192 \pm 6\ \mu\mathrm{m}$	$\sigma_{\text{cell}} \approx 231\ \mu\mathrm{m}$

Table 1: *This Table summarizes the widths of the residuals for a single layer. The distinction between cosmic data and prediction from simulation with magnetic field is made, as well as the comparison whether the probed layer is included in the calibration- and segment-fit or not. Note that the true cell hit resolution is expected to be in-between, see last column (obtained by applying certain correction factors).*

Besides the performance of the segment-reconstruction in terms of resolution, Fig. 10 displays the distribution of the number of hits contributing to a segment. The amount of hits used to create a combined Superphi-segment and a θ-segment is shown there for data and simulation in comparison. One can see that hardware and software show very good results since in most cases 8 hits and 4 hits respectively can be measured by the chamber and combined to form a segment. As one would expect in the simulation the efficiency for this ideal case is a bit higher than in the data, where one or more hits are lost more often or layers with multiple hits may contribute. These multiple hits can araise from secondaries or noise. Still the measured and the predicted performance is quite comparable. Also note that for all events the trigger conditions as defined earlier are required (see Sect. 6). This explains why in the case of the Superphi-combination only a small number of segments with < 7 hits can be found.

7.2 Results from cosmic track-reconstruction

As introduced in Sect. 6 the different chamber measurements can be combined performing a track-fit. The track parameters such as angle and momentum of the cosmic muon can be accessed at the innermost muon station after both forward- and backward-fit have been applied. As always only events fulfilling the trigger conditions are analysed as discussed in Sect. 6. No further selection cuts have been applied in order to select only high quality tracks. The tracks are simply required to fulfill some loose χ^2-cuts (30000 for forward-fit using 3D-segments, 100

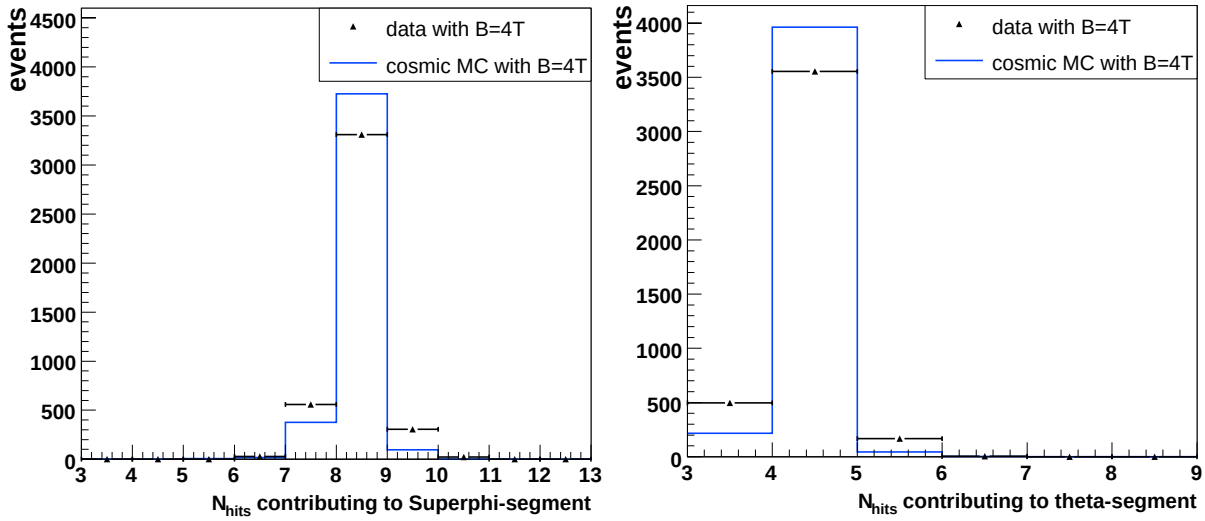

Figure 10: *In order to study the performance of the local reconstruction the number of hits contributing to the chamber segments are displayed here, for data and simulated events in comparison as seen by MB3 in Sector 10 of YB+2 with magnetic field. The left plot corresponds to the combined Superphi-segment and the right one to the measurement of the single θ-Superlayer.*

for backward-fit using cell hits) and that at least 2 Drift Tube chambers contribute. Comparing distributions in data and in simulation again the Monte Carlo prediction can be validated and by looking at track-parameters the performance of the tracking software can be tested. In general the results from the Cosmic Challenge represent the first time where real tracks can be measured with the CMS detector and can even be reconstructed, including the influence of the magnetic field and using the official software packages.

The first important number is the average efficiency of the track-reconstruction: In the data as well as simulated events with magnetic field the CosmicMuonProducer can find tracks with an average efficiency of

$$\varepsilon\,(\text{track-reconstruction}) \approx 97\% \tag{8}$$

for the triggered events. Only less than 1‰ of the events in data and in simulation have more than one cosmic track, caused by noise, segment ambiguities or by two real cosmics in coincidence. These efficiencies demonstrate impressively the good performance of the cosmic track finder.

Figures 11 and 12 show the tracking angles at the innermost measurement φ_{track} and ϑ_{track} as defined in Fig. 7. Again the data are normalized to the lower Monte Carlo statistics and the dropping of the trigger-efficiency at large angles is included in the simulation. Just like in the case of local reconstruction also at the tracking-level the simulation nicely reproduces the shape of the measured distributions, both with and without magnetic field. Also the physical content of the plots stays within expectations: The φ_{track}-distribution is peaked around -90° which corresponds to a vertical cosmic muon coming from above. Also in ϑ_{track} a peak around 90° can be observed in the measured and simulated events, again since vertical cosmic muons are expected to dominate. Due to the specific acceptance of the MTCC-Drift Tube setup a non-Gaussian and asymmetric behaviour can be seen. Especially in φ the staggering of the chambers relative to each other and the fact that the inclined sector 11 is active leads to the patterns in this figure. In the φ-plane the bending of the magnetic field takes place and causes some differences between the left and the right plot. But just as in the case of local reconstruction, the biggest effect of the magnetic field is the drop in statistics as less cosmic muons reach the bottom sectors and form a track there.

In order to test the correctness of the track-reconstruction the measured angles can be compared with the information obtained from simulation. During the detector simulation the muons are propagated through the detector material, accounting for the interaction with the magnetic field and with the hardware material. The angle at the innermost tracking-measurement can be compared to the "true" angle of the simulated muon inside the same cell. This is shown in the left plot of Fig. 13 where the difference between simulated and reconstructed φ_{track} is displayed

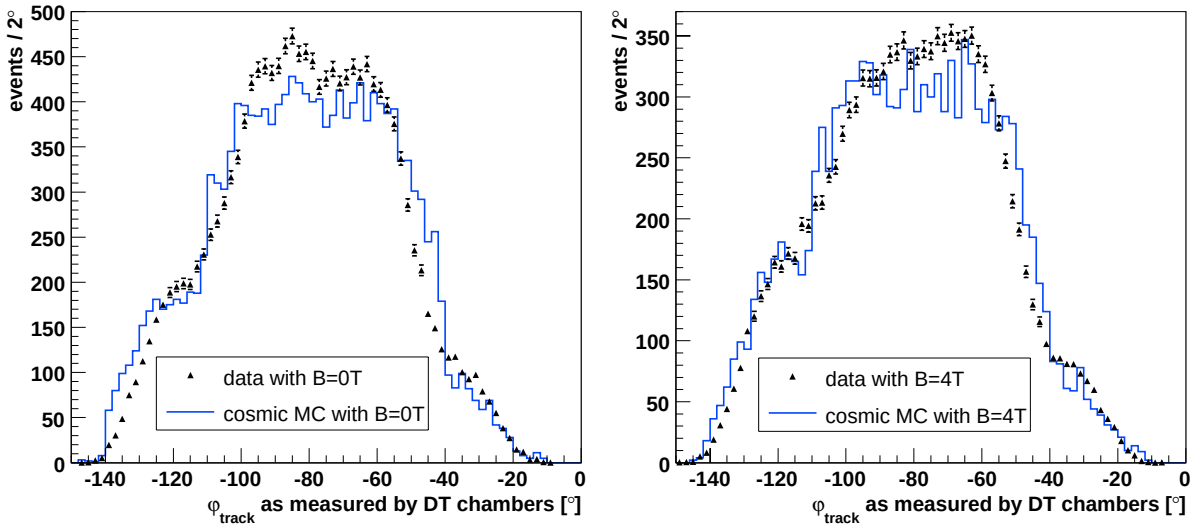

Figure 11: *The angle φ_{track} at the innermost measurement of the cosmic muon track is shown here, for simulation (continuous line) and data (triangles, normalized to MC statistics) in comparison. The left plot corresponds to the case without magnetic field, the right plot to* 4 T *within the solenoid.*

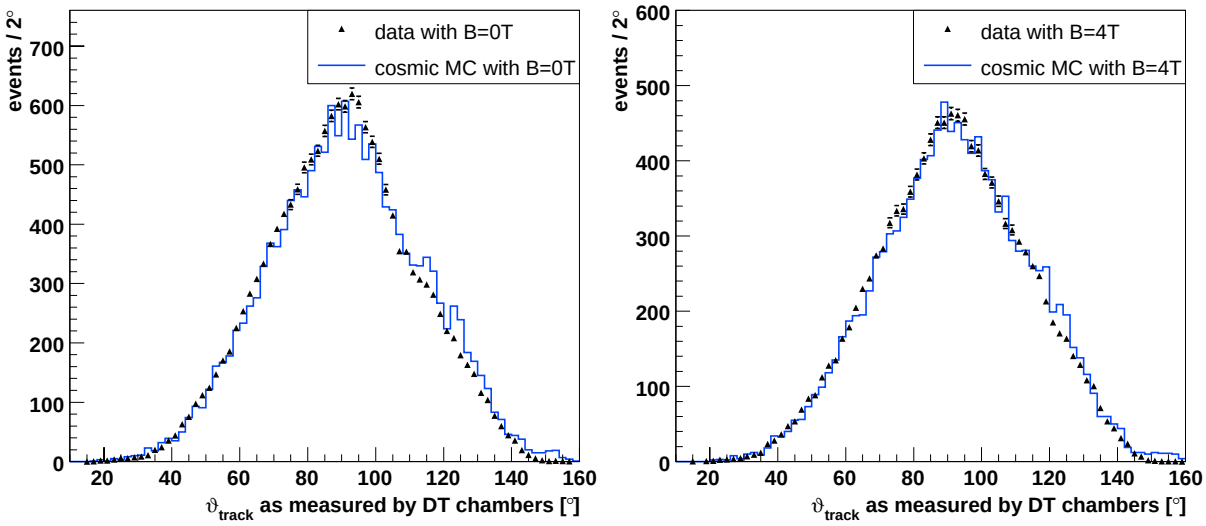

Figure 12: *The angle ϑ_{track} at the innermost measurement of the cosmic muon track is shown here, for simulation (continuous line) and data (triangles, normalized to MC statistics) in comparison. The left plot corresponds to the case without magnetic field, the right plot to* 4 T *within the solenoid.*

for the Monte Carlo sample with magnetic field. Since measurement and true value are compared at the same place the magnetic field or multiple scattering do not affect this difference. One can see a narrow Gaussian distribution which is centered at zero, thus in most cases the cosmic muon is measured correctly. The width amounts only 0.1 ° which means that the cosmic tracks are reconstructed very precisely.
The right plot of Fig. 13 compares the amount of cell hits contributing to the track-fit in data and in Monte Carlo events. The prominent peaks correspond to 24 hits, 32 hits, 36 hits and 44 hits; MB1, MB2 and MB3 can contribute with 12 hits at most while MB4 only contains 8 layers, thus the combination of the different chambers explains this pattern. Since a cosmic muon crosses the detector setup coming from all directions not all four muon stations are hit in each event. Comparing the data with the Monte Carlo prediction one can see that the ideal case of two, three or four crossed Drift Tube chambers with all layers hit is present less often in the real measured tracks. Hits may get lost or additional hits due to noise may contribute. Note that alignment corrections have not been applied in the data yet and thus displaced hits might not match with the remainder measurements.

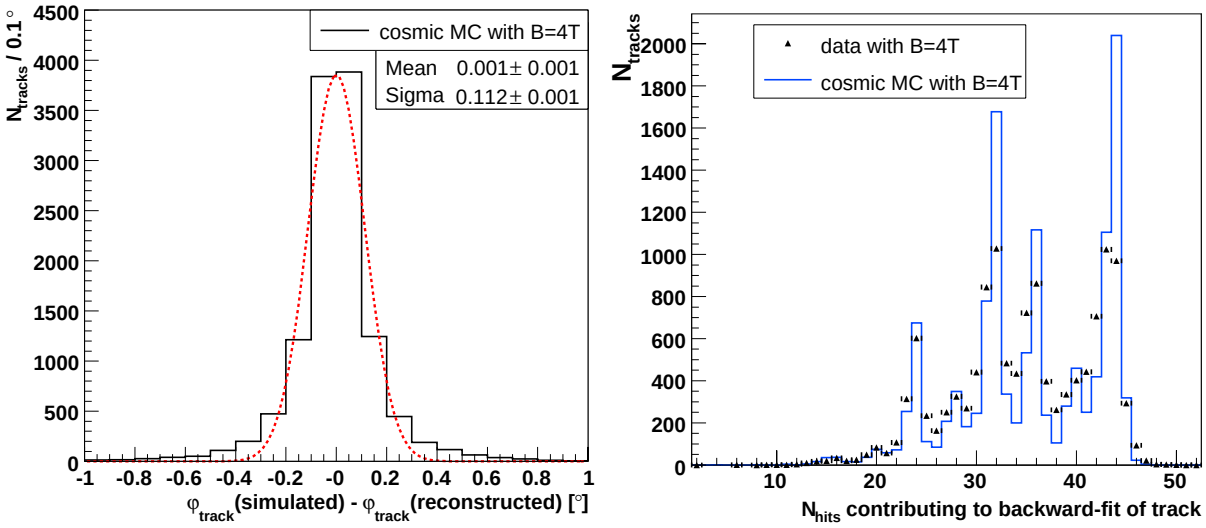

Figure 13: *Here the performance of the cosmic track-reconstruction is studied. The left plot shows the difference between simulated and reconstructed φ_{track}-angle at the innermost measurement for simulated events with magnetic field; a Gaussian fit is performed. The simulated information is taken from the detector simulation at the position of the innermost track measurement. The right plot compares the amount of hits which contribute to the final track-fit in data and simulated events with magnetic field.*

In Fig. 14 one can see how the different muon stations contribute to the track-finding when a magnetic field is present. Displayed here are the amount of cell hits used for the backward-fit. The different bins in x correspond to the different chambers MB1-MB4, one group of bins consists of sector 10 in YB+1, the next of sector 10 in YB+2 and the last peak of sector 11 in YB+2. Note that in both sector 10 two MB4 are present (the second MB4 is assigned to sector 14) which explains the two apart standing peaks. In general the simulation describes the distribution of the hits as seen in the data quite accurately. Consistent with the numbers from local reconstruction also here an equal amount of tracks is found in each sector of the MTCC-setup. The cosmic track-reconstruction is also quite efficient for inclined sectors such as sector 11. In most events hits from MB2 and MB3 are used since these two chambers are required to contain signals by the trigger. This underlines again the importance of modeling the trigger-conditions also in the simulated events.

The results so far demonstrate that it is possible to reconstruct cosmic muon tracks, with and without the 4 T magnetic field. Of course this suggests to also investigate the design motivation why the CMS detector has such a strong magnetic field at all: The transverse momenta of the particles are to be measured. Figure 15 addresses this issue since the p_T of the cosmic muons as seen at the innermost point of the track is shown here. The upper plot displays the low-momentum region and the lower plot refers to cosmic muons with higher p_T, in both distributions the data are normalized to the simulated events only in the range visible in the plots ($f_{\text{scale}} = 0.142$ for upper plot, $f_{\text{scale}} = 0.099$ for lower plot).
The shape of the distribution is as expected since cosmic muons follow a steep declining energy dependence (see Sect. 3). In addition to this the agreement between data and Monte Carlo prediction is reasonable. Data and MC distributions have their maximum at some minimal momentum of $2-4$ GeV; muons with even smaller momentum do not cross enough active detector material to form a track candidate. In general the shape of the distribution is reproduced nicely by the simulation. Also the high-p_T tail is described properly, normalizing only to the events above 30 GeV. Both plots show that the energy dependencies assumed in the cosmic generator are correct and that the track-reconstruction performs similar in data and simulation. Looking at the upper plot the Monte Carlo curve appears to be narrower than the measured one, leading to a MC excess at small momenta and less populated high-p_T tail. This could be caused either by the fact that no alignment corrections have been applied in the data or by an overestimation of the assumed resolutions in the detector simulation, as well as a miscalibrated momentum scale. Small momenta are also affected by the lower energy cut of 7 GeV during generation. In the data some cosmic muons with smaller momenta might also produce track-candidates. Also, as mentioned before, the trigger

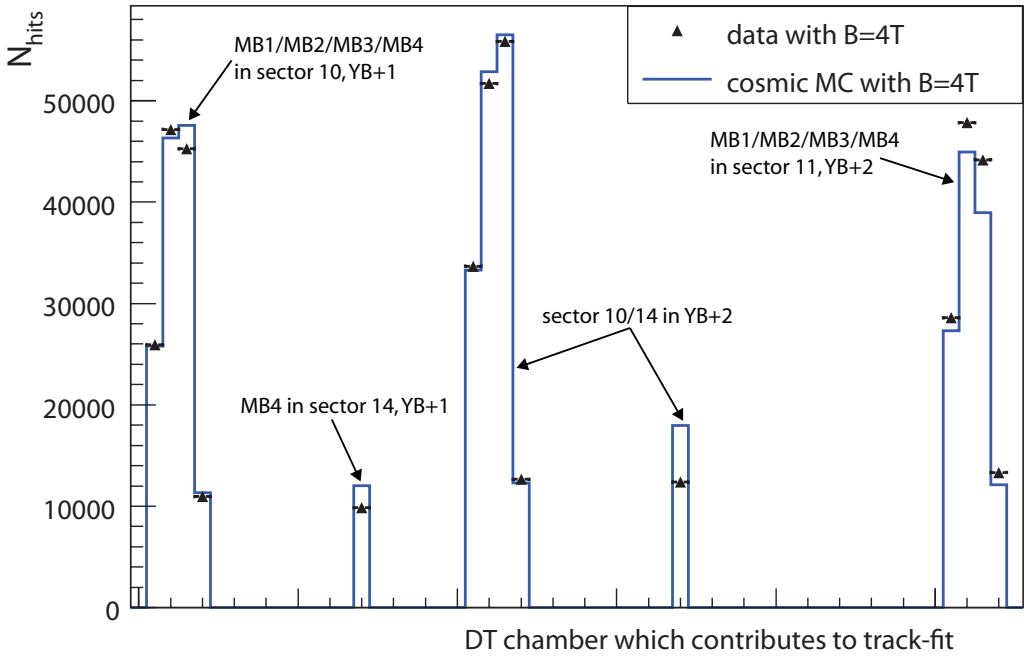

Figure 14: *The plot illustrates how often the different DT chambers of the MTCC-setup contribute with hits to the track-fit. Each bin in x which has an entry corresponds to a specific chamber. Data and Monte Carlo prediction with magnetic field are compared to each other. One can see that in general all 3 sectors are illuminated equally.*

conditions are only modeled approximately in the simulation. All these points, as well as the instrinsic uncertainty of the cosmic generator, make clear that there are differences to be expected between data and Monte Carlo which might affect the level of agreement in the p_T-distribution. Trigger and 7 GeV cut have especially an impact on the low momentum region (upper plot). At high-p_T the trigger-efficiency should become flat in energy and an energy cut in the generation has only little influence. Thus in the lower plot missing alignment corrections and the unknown momentum-resolutions and absolute momentum-scale dominate the uncertainties of the measurement.

The next step is to investigate the quality of the p_T-measurement. This can be easily done using the Monte Carlo sample since the simulated information can be compared to the reconstructed one. The left plot of Fig. 16 shows the difference between simulated and reconstructed p_T. Again the simulated hit-information at the position of the innermost track-measurement is used to obtain the "true" p_T-value. A Gaussian fit is performed and both mean and sigma show that when using cosmics the momentum can be estimated from the track.
An assessment of the performance of the momentum measurement can be extracted from the right plot of Fig. 16. Since the measured quantity is the sagitta s of the track where $s \propto 1/p_T$, and since $\frac{\Delta(1/p_T)}{1/p_T} = \frac{\Delta p_T}{p_T}$, the sigma of the Gaussian fit shown corresponds to the p_T-resolution. So using the MTCC-setup and the cosmic track finder the simulation predicts a relative p_T-resolution of 24%. This value can be compared to the results of Standalone muon reconstruction, i.e. Muon System only, as stated in the Technical Design Report [21]: Here a p_T-resolution of $\approx 10\%$ is expected for 10 GeV muons from pp-collisions and measured by the barrel Muon System. The difference can be explained by the peculiarities of cosmic muons, i.e. their timing uncertainty and the lack of a vertex constraint.

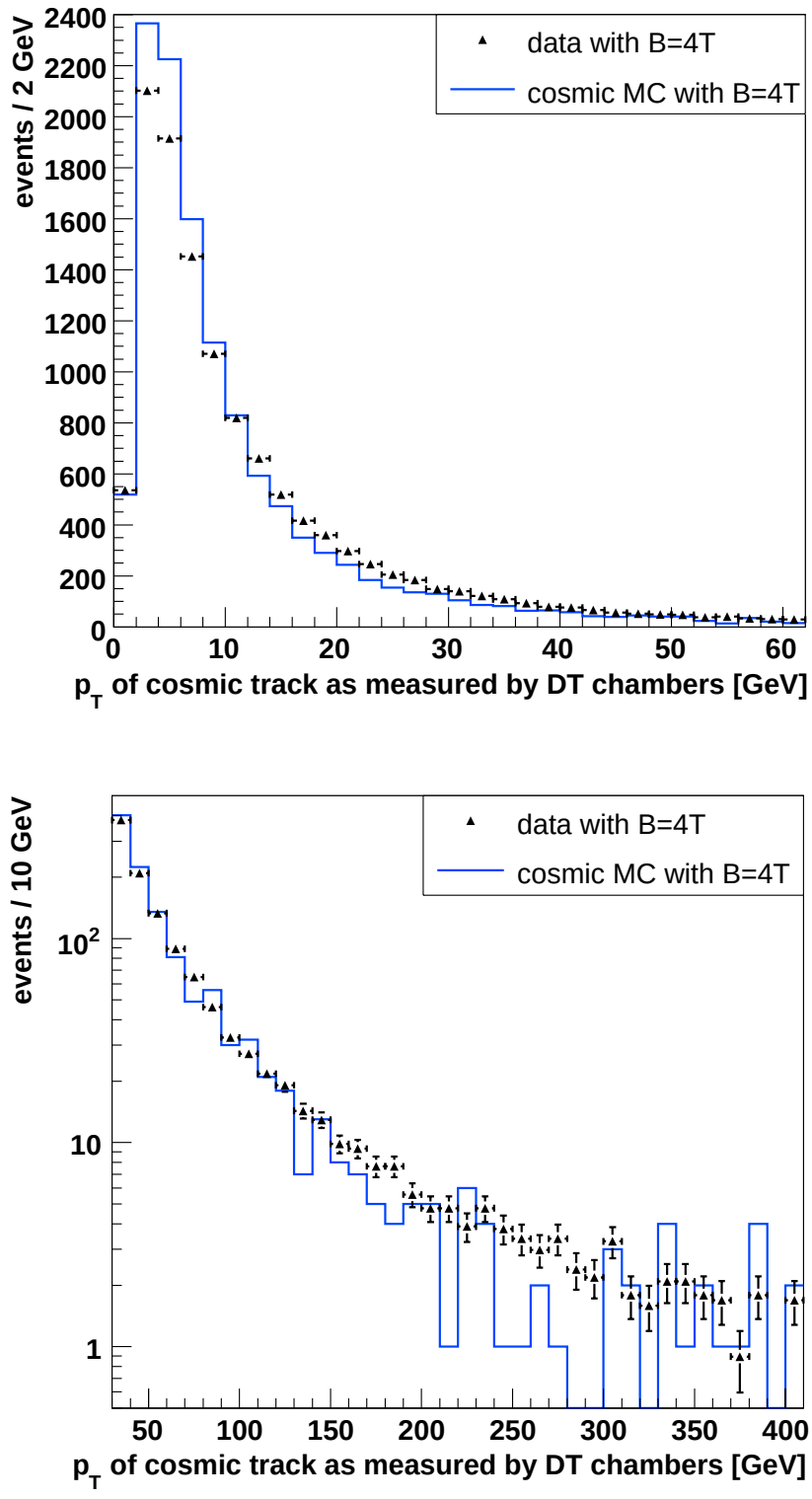

Figure 15: *The p_T-distribution at the innermost measurement of the cosmic muon track is shown here, for simulation (continuous line) and data (triangles, normalized to MC statistics in the range displayed). Note that in the low-p_T region (upper plot) differences might arise from the fact that in simulation a lower threshold of $E_{gen} > 7$ GeV is used and no full trigger-simulation is run. In the high-p_T tail (lower plot) the important fact is that no alignment-corrections have been applied to the data and that a calibration of the momentum-resolution and absolute momentum-scale is missing.*

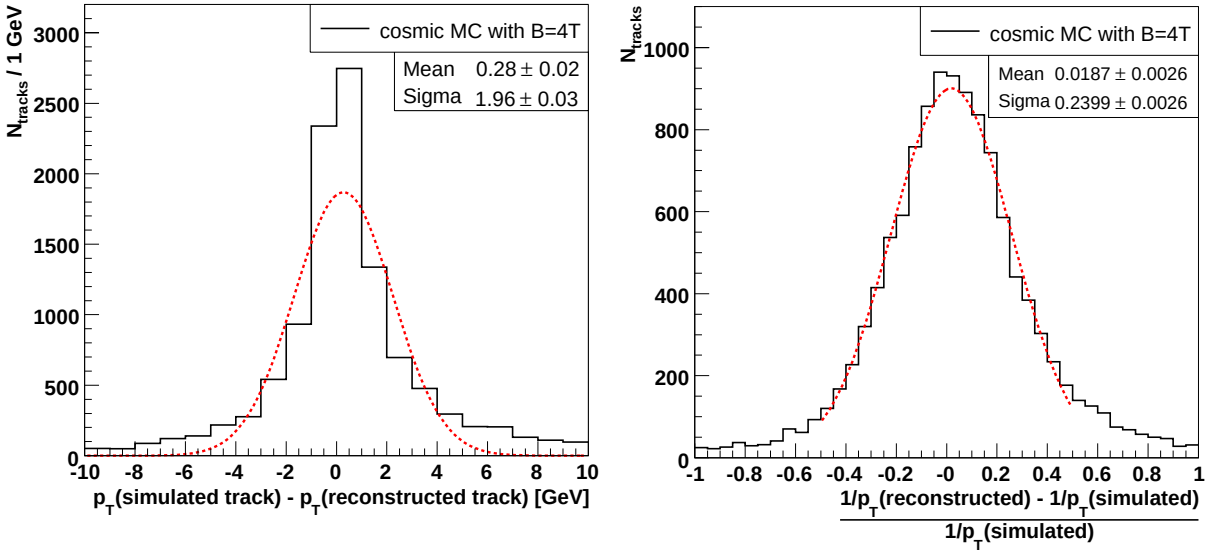

Figure 16: *The quality of the p_T-measurement is studied here, using the simulated sample with magnetic field. The left plot shows the difference between simulated and reconstructed p_T-value at the innermost measurement, a Gaussian fit is performed. The simulated information is taken from the detector simulation at the position of the innermost track measurement. In the right plot the reconstructed and simulated information is used to compute $\Delta(\frac{1}{p_T})/\frac{1}{p_T}$. The widths of the Gaussian fit corresponds to the p_T-resolution when measuring cosmic muons with the DT chambers only, without any vertex constraint applied.*

7.3 Multiple scattering, charge ratio and rate estimates

The effect of multiple scattering:

At low momenta the resolution of the track-measurement is mainly limited by the effect of multiple scattering of the cosmic muons inside the iron of the magnetic flux return yoke and the hadronic calorimeter. Thus an important check of the precision of the track-reconstruction is to test whether the observed measurements are compatible with the uncertainties caused by multiple scattering.
In this context Fig. 17 compares the generated angle ϑ_{track} with the reconstructed one. As the cosmic muons are generated on a cylinder outside the CMS detector and are mainly reconstructed at the place of MB1/MB2 in the bottom sectors 10 and 11 of the MTCC-setup, the cosmic muons have to pass through a well defined material volume of ≈ 330 radiation lengths [22]. This yields a diversion in the angle due to multiple scattering of

$$\Delta\vartheta_{track} \approx \frac{13.6\ \text{MeV}}{5\ \text{GeV}}\sqrt{330} = 2.8^\circ \qquad , \tag{9}$$

see [23]. Since the generated cosmic muons have a minimal energy of 7 GeV and since they loose further energy on their way through the detector material, 5 GeV is assumed in this rough estimate. In the left plot of Fig. 17 a double Gaussian fit is performed on the difference of generated and reconstructed angle. This fit accounts for the larger tails which are typical of multiple scattering processes. Note that in the ϑ-plane the cosmic muons are not affected by any bending within the magnetic field, thus the distribution has a mean centered around zero. The widths of the first Gaussian is $\approx 2.8^\circ$ which means that the results of the track algorithm are well compatible with the limitations given by multiple scattering.

Within one sector of the MTCC-setup one can also investigate the multiple scattering effects between two fixed muon stations, e.g. between MB1 and MB3. Again in the ϑ-plane only the material of ≈ 50 radiation lengths [22] can cause deviations in the angles, not the magnetic field. This results in an expected diversion in the angle of

$$\Delta\vartheta_{track} \approx \frac{13.6\ \text{MeV}}{5\ \text{GeV}}\sqrt{50} = 1.1^\circ \qquad , \tag{10}$$

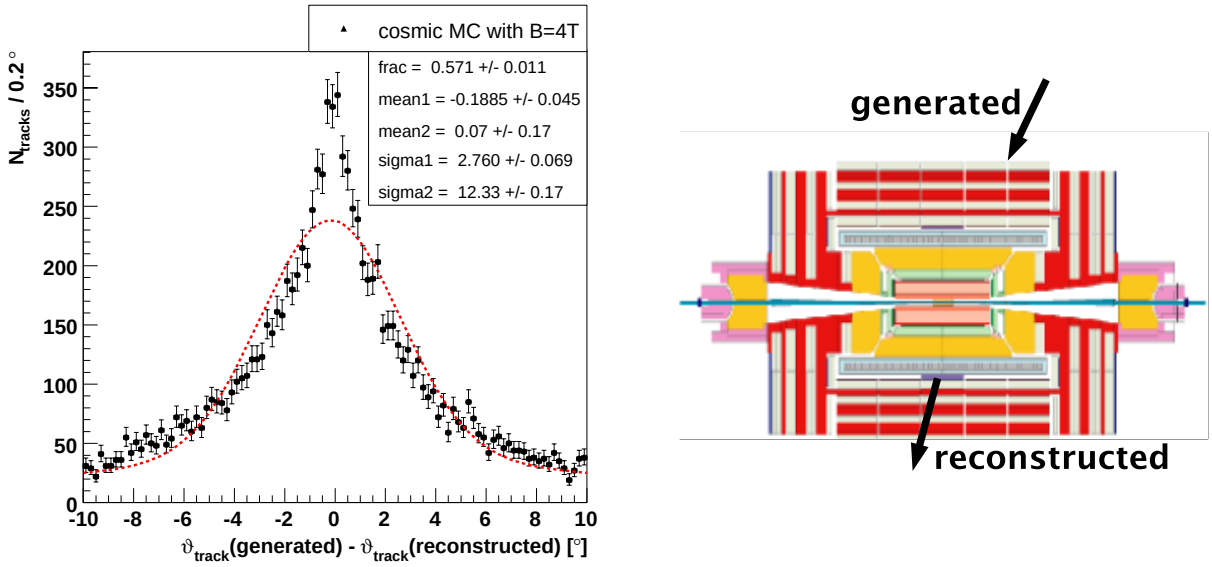

Figure 17: *Left: The difference between generated ϑ_{track} and the one reconstructed at the innermost measurement is shown, using simulated cosmics with magnetic field. A diversion in the angle is expected from multiple scattering effects and a double Gaussian fit is performed to account for the long tails.*
Right: Illustration of where generated and reconstructed angles are located.

assuming a mean cosmic energy of 5 GeV. This expectation can now be compared with the reconstructed difference as seen in data and in simulated events. In addition to this the measurements from local chamber reconstruction, i.e. before any track-fit has been performed, can be compared to the results obtained from track-reconstruction. All these issues can be seen in Fig. 18, here for the samples with magnetic field. The left column corresponds to the data, the right depicts the Monte Carlo expectation. The two upper plots show the difference of the ϑ_{track}-angles as observed by the chamber segments of local reconstruction in MB1 and MB3. Again a double Gaussian-fit has been performed to account for the long multiple scattering tails. The sigmas of the first Gaussian of both data and Monte Carlo are around $1.8\,^{\circ}$, so only slightly larger than the estimated $1.1\,^{\circ}$. The two bottom plots now represent the measurements after the track-fit has been performed (innermost measurement=MB1, outermost measurement=MB3). Note that the scale on the x-axis has shrunken, thus the distributions are much narrower. Both data and Monte Carlo prediction have $\sigma_1 \approx 0.7^{\circ}$, thus the fitting procedure largely improves the measurement. In general the performance of the track-reconstruction seems to be very comparable in data and in simulated events, only the bottom data distribution reveals a slight offset in the mean of the inner Gaussian not reproduced by the detector simulation. Again influences of the missing chamber alignment could explain this.

Measuring the charge of cosmic muons:

As the p_T-measurement is based on the curvature of the cosmic muon track caused by the magnetic field present in the iron return yoke, the charge of the muon can be determined from the sign of the curvature. In the simulated events the knowledge of the "true" charge can be used in order to estimate the charge misidentification probability. Averaged over all momenta and angles of the generated cosmic muons the Monte Carlo sample predicts a probability of

$$p\,(\text{charge misidentification}) = 0.036 \pm 0.002 \qquad . \tag{11}$$

In [21] a value of 0.001 is stated for 10 GeV standalone-muons from pp-collisions, here using a vertex constraint. Still the 4% observed with cosmic muons is a promising results, especially as additional track-quality cuts can further improve this value. Note that in order to obtain these results a small fix in the CosmicMuonProducer code of the CMSSW version used had to be performed which eliminates unphysical charge-flips during reconstruction.

This low charge misidentification probability shows that in principle the charge of the cosmic muons can be measured correctly. Before presenting the results one should remember the natural charge ratio of cosmic muons $N_{\mu+}/N_{\mu-} \approx 1.3$, see Sect. 3. In this part of the study only tracks reconstructed in the two horizontal sectors 10 are used in order to ensure a more symmetrical detector setup.

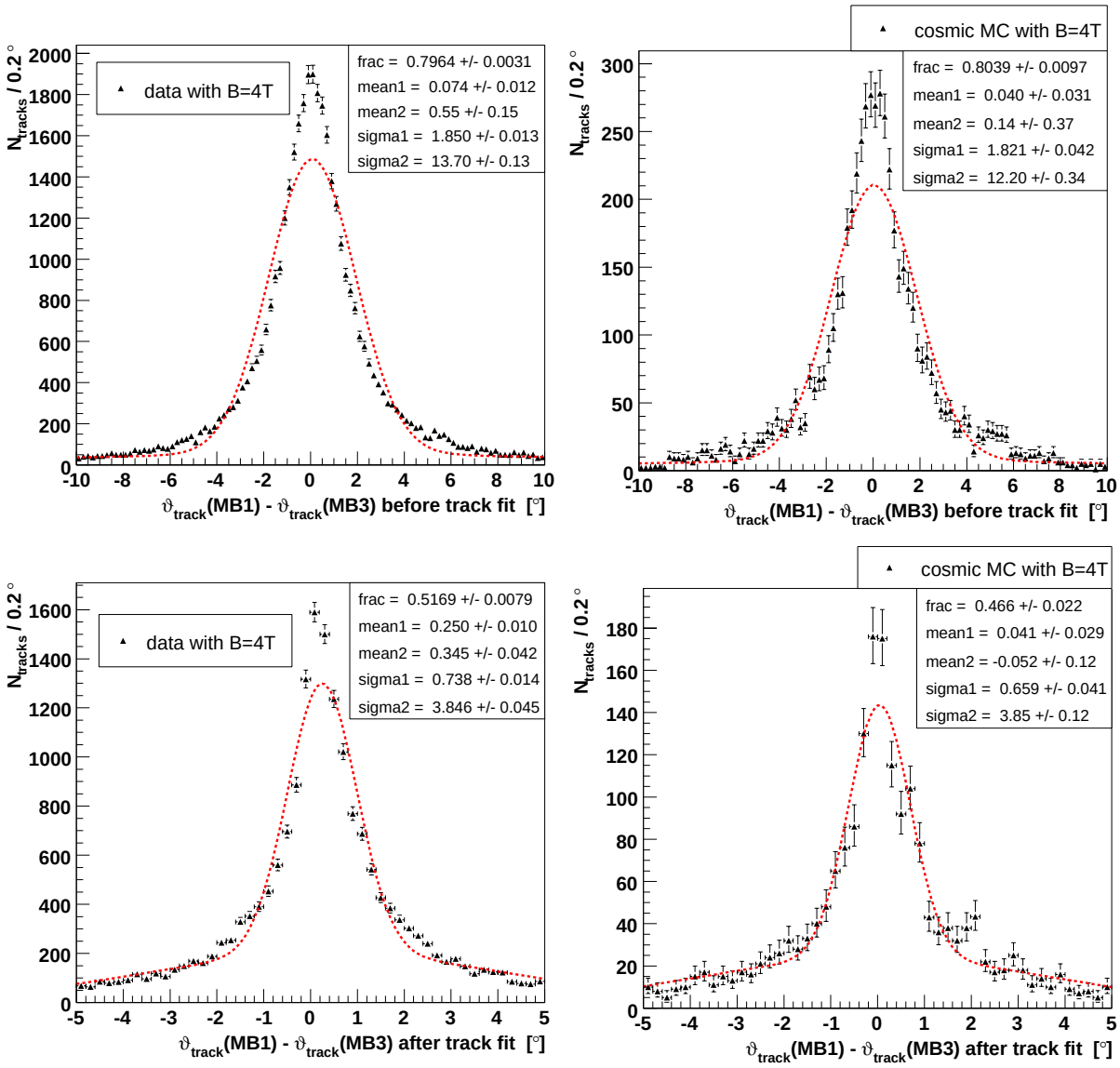

Figure 18: *Differences in ϑ_{track} due to multiple scattering are investigated at two distinct places (between MB1 and MB3). The left column refers to data with magnetic field and the right to the MC prediction. The two upper plots display the difference in the angle at chamber reconstruction level, thus the difference for the segments before a track-fit is performed, and the bottom plots the final track-angles where innermost and outermost measurement correspond to MB1 and MB3 respectively. In all cases a double Gaussian fit is performed accounting for the long tails.*

The results of the charge measurements and the corresponding expected values are summarized in Tab. 2, again averaged over all occurring momenta and angles. Note that for the reconstructed tracks the ratio is corrected for the charge misidentification probability of $\varepsilon = 3.6\%$ mentioned above, assuming

$$N^+(\text{true}) = N^+(\text{meas}) \cdot (1-\varepsilon) + N^-(\text{meas}) \cdot \varepsilon \qquad . \tag{12}$$

The errors are statistical only.

One can see that in the simulation the charge ratio which is an output of the cosmic generator and the ratio obtained by the track-reconstruction, using sector 10 only, are well within their errors. Also the ratio reconstructed in the data is very similar to the one obtained with the Monte Carlo sample (line 3). Still the measured ratio of 1.35 is higher than the one expected from previous measurements (1.27 for vertical and 10 GeV muons only), and the ratio reconstructed in the Monte Carlo sample (1.35) is higher then the output of the generator (1.33). This could be due to the specific (asymmetric) acceptance of the MTCC-setup and the influence of the magnetic field inside the CMS detector which might enhance a particular charge.
In general, all values are compatible with a charge ratio of ≈ 1.3.

	data events	Monte Carlo events
$\frac{N_{\mu+}}{N_{\mu-}}$(generated) for all events		1.33
$\frac{N_{\mu+}}{N_{\mu-}}$(generated) for events with track		1.32 ± 0.03
$\frac{N_{\mu+}}{N_{\mu-}}$(reconstructed) for events with track	1.35 ± 0.01	1.35 ± 0.03
$\frac{N_{\mu+}}{N_{\mu-}}$ from independent measurements for vertical and 10 GeV muons only [11]	1.27 ± 0.01	

Table 2: *Summary of generated, reconstructed and measured values of the cosmic muon charge ratio. The reconstructed values in simulated and measured events with magnetic field are corrected for a charge misidentification probability of* 3.6% *and can be compared to each other (line* 3*), while line* 2 *states the "true charge ratio" of the reconstructed tracks within the simulation.*

Comparison of measured and predicted rates:

Another task of CMSCGEN is the prediction of rates of cosmic muons arriving at certain sub-detector parts (see Sect. 3), for example, potentially available for detector alignment. Cosmic ray muons may also constitute a background in the search for rare physics processes during pp-collisions. The predicted rates can be compared to the trigger rates measured with the Drift Tube MTCC setup. Such comparisons help to validate the Monte Carlo prediction and qualifies the performance of the trigger setup used during the Cosmic Challenge.

The DT trigger-rates during MTCC data taking can be deduced from the Run Summary Web Page. The efficiency of the trigger may vary at the level of a few percent thus adding a systematic uncertainty. Also the predicted rates have some uncertainty, largely caused by the modelling of the trigger conditions as described in Sect. 6. While the DT trigger efficiency has been determined to be $\approx 90\%$ with a bunched muon testbeam [24], with cosmic muons the average DT trigger efficiency has been measured to be only $\varepsilon_{\text{trigger}} = 40 - 50\%$ [25], varying from run to run. The low efficiency is attributed to the non-syncronization of cosmic muons with the trigger clock. This causes an increased probability of poor quality triggers and of muons assigned to a neigbouring bunch crossing. This number of trigger efficiency is a rough estimate for the trigger configuration used in the two runs analyzed for this study. It has been applied as a constant factor to correct the predicted Monte Carlo rates accordingly.

The comparison between the DT trigger rates as measured in the two particular MTCC runs used in this analysis and the ones predicted by simulation (including the modelling of the trigger conditions as discussed before) are summarized in Tab. 3. The DT trigger for these two runs included only MB2 and MB3 stations in the three MTCC sectors. The second column of the table refers to the predicted rates after correction for a trigger efficiency of $40 - 50\%$. The third column states the original predicted rates, the errors include statistical and some systematic contributions, following Equations 2 and 3.

	measured DT-trigger rates	predicted DT-trigger rates $\times\ \varepsilon_{\text{trigger}}$	predicted DT-trigger rates
$B = 0$ T	90 Hz	$105 - 130$ Hz	262 ± 2 (stat.) ± 18 (syst.) Hz
$B = 4$ T	70 Hz	$80 - 100$ Hz	202 ± 2 (stat.) ± 14 (syst.) Hz

Table 3: *Comparison of the cosmic muon trigger rates as predicted by CMSCGEN with the trigger rates measured by the Drift Tube MTCC trigger configuration with MB*2 *and MB*3 *stations participating in the DT trigger. The rates without magnetic field (first line) are slightly higher than with magnetic field (second line) due to bending of low momentum muons out of the acceptance. Rates in the second column are already corrected for an assumed trigger-efficiency of* $40 - 50\%$*, in the last column the errors of the original prediction are stated.*

In general, data and Monte Carlo prediction (corrected for $\varepsilon_{\text{trigger}}$) have a value consistent with 100 Hz, thus the simulation of the cosmic muon rates gives results in the correct order of magnitude. Both also show the trend towards lower trigger rates with the magnetic field being present. Still, the measured rates are lower by a

factor of $0.7 - 0.9$. This could be related to the modelling of the trigger conditions rather than using a detailed simulation of the specific MTCC trigger setup which had to be modified with respect to its design for pp-collisions. The fact that the predicted trigger rates without the efficiency correction are much higher than the measured ones, is yet another indication that the measured low efficiency is correct for the case of cosmic muons and support the identified reason related to the timing uncertainty of the incoming cosmic muons. In summary, the cosmic simulation is well suited to predict rates quite precisely, allowing reliable cosmic rate estimates for future tests and studies.

8 Summary

In summary, at all levels of reconstruction the comparison of cosmic muons from MTCC with the predictions made by the cosmic generator CMSCGEN shows very promising results. This demonstrates that the assumed angular- and energy-dependencies within the cosmic generator are correct, and that the detector simulation within the CMS software can describe the data quite precisely.
The analysis of the MTCC data show that the CMS experiment can indeed be operated in a stable mode, including a magnetic field. Physics objects up to tracks can be reconstructed correctly in MTCC data as well as Monte Carlo events using the barrel Muon System. The extraction of cosmic muon properties from simulated data allows to study the performance of reconstruction algorithms and their measurement precision. These results meet or even exceed the expectations for non-bunched muons so far. Moreover, cosmic muons are anticipated to be used for synchronization and alignment purposes in the future. All this underlines that cosmic muons are the ideal source to study the detector performance during the commissioning of CMS and the early days of LHC-running, ranging from basic operation tests up to high definition objects such as tracks.

Acknowledgments

Many thanks to Nicola Amapane, Riccardo Bellan, Sara Bolognesi, Michael Bontenackels, Gianluca Cerminara, Albert De Roeck, Maria Cruz Fouz, Ugo Gasparini, Chang Liu, Anna Meneguzzo, Martijn Mulders, Norbert Neumeister and Marco Zanetti for their continuous support and for providing detailed information which was very helpful for this work. Special thanks to Carsten Hof and the Aachen/Desy GRID Team for providing the tools and infrastructure to generate the simulated samples. In addition to this we would like to express our gratitude to the many people involved in operating the detector during MTCC, especially our colleagues carrying out the many DT shifts. Many thanks to Daniel Francois Teyssier, Begona De La Cruz and Chiara Mariotti for carefully reviewing this manuscript. Work supported in part by BMBF and DFG.

References

[1] CMS Technical Design Report “The Muon Project”. CERN/LHCC 97-32, CMS TDR 3, 15 December 1997.

[2] CMS Technical Design Report “The TriDAS Project, Volume 1: The Trigger Systems”. CERN/LHCC 2000-38, CMS TDR 6.1, 15 December 2000.

[3] V. Drollinger. “Simulation of Beam Halo and Cosmic Muons”. CERN CMS NOTE 2005/012.

[4] E. Barberis, P. Biallass, V. Drollinger, K. Hoepfner, D.R. Wood. “Trigger and Reconstruction Studies with Beam Halo and Cosmic Muons”. CERN CMS NOTE 2006/012.

[5] P. K. F. Grieder. “Cosmic Rays at Earth: Researcher’s Reference Manual and Data Book”. Amsterdam, Netherlands: Elsevier (2001).

[6] T. Hebbeker, A. Korn. “Simulation Programs for the L3+Cosmics Experiment”. L3-C note, 1998. `http://web.physik.rwth-aachen.de/~hebbeker/l3csim.pdf`.

[7] O. Adriani et al. “The L3+C detector, a unique tool-set to study cosmic rays”. Nucl. Instrum. Meth. A **488** (2002) 209.

[8] D. Heck, J. Knapp et al. “CORSIKA: A Monte Carlo Code to simulate Extensive Air Showers”. Forschungszentrum Karlsruhe, Report FZKA 6019, 1998.

[9] P. Achard et al [L3 Collaboration]. “Measurement of the atmospheric muon spectrum from 20-GeV to 3000-GeV”. Phys. Lett. B **598** (2004) 15.

[10] M. Unger. “Measurement of the muon momentum spectrum of atmospheric muons with the L3 Detector”. PhD thesis, Humboldt University Berlin, 2003.

[11] T. Hebbeker and C. Timmermans. “A Compilation of High Energy Atmospheric Muon Data at Sea Level”. Astropart. Phys. 18 (2002) 107.

[12] J. Allison et al. “Geant4 developments and applications”. IEEE Trans. Nucl. Sci. 53 (2006) 270.

[13] N. Amapane et al. “Local Muon Reconstruction in the Drift Tube Detector”. CERN CMS NOTE in preparation.

[14] “The SQLite Web Page”. `http://www.sqlite.org/`.

[15] J. Puerta-Pelayo, M.C. Fouz, P. Garcia-Abia. “Parametrization of the Response of the Muon Barrel Drift Tubes”. CERN CMS NOTE 2005/018.

[16] “The IGUANA Web Page”. `http://iguana.web.cern.ch/iguana/`.

[17] A.T. Meneguzzo et al. “Method for the Measure of the Time of the Track Passage and of the Drift Velocity in the Drift Tube Chambers of CMS”. CERN CMS NOTE in preparation.

[18] S. Bolognesi et al. “Measurment of Drift Velocity in the CMS Barrel Muon Chambers at the CMS Magnet Test Cosmic Challenge”. CERN CMS NOTE in preparation.

[19] C. Liu, N. Neumeister. “Cosmic Muon Reconstruction and Analysis”. CERN CMS NOTE in preparation.

[20] R. Frühwirth. “Application Of Kalman Filtering To Track And Vertex Fitting”. Nucl. Instrum. Meth. A **262** (1987) 444.

[21] CMS Physics TDR, Volume 1 “Detector Performance and Software”. CERN/LHCC 2006-001, 2 February 2006, Figure 9.3/9.4.

[22] CMS Physics TDR, Volume 1 “Detector Performance and Software”. CERN/LHCC 2006-001, 2 February 2006, Figure 1.3.

[23] W-M Yao et al. “Review of Particle Physics”. 2006 J. Phys. G: Nucl. Part. Phys. 33, Equation 27.12.

[24] P. Arce et al. “Bunched beam test of the CMS drift tubes local muon trigger”. Nucl. Instrum. Meth. A **534** (2004) 441.

[25] F.R. Cavallo, P. Zotto. “Private communication”.